LXR-inducible host E3 ligase IDOL targets a human cytomegalovirus reactivation determinant to promote latency

Luwanika Mlera[1,2], Donna Collins-McMillen[1,2], Sebastian Zeltzer[1,2], Jason C. Buehler[1,2†], Melissa Moy[3†], Kristen Zarrella[1], Katie Caviness[1,2,4§], Louis Cicchini[2,5¶], David J. Tafoya[1,2], and Felicia Goodrum[1,2,3,5*]

[1]Department of Immunobiology, University of Arizona, Tucson, AZ 85721, USA

[2]BIO5 Institute, University of Arizona, Tucson, AZ 85721, USA

[3]Graduate Interdisciplinary Program in Cancer Biology, University of Arizona, Tucson, AZ 85721, USA

[4]Graduate Interdisciplinary Program in Genetics, University of Arizona, Tucson, AZ 85721, USA

[5]Department of Molecular and Cellular Biology, University of Arizona, Tucson, AZ 85721, USA

[†]Current address: Imanis Life Sciences, Rochester, MN 55901, USA

[§]Current address: National Biodefense Analysis and Countermeasures Center, Fort Detrick, MD 21702, USA

[¶]Current address: PPD, Inc., 929 N Front St. Wilmington, NC 28401, USA

***Correspondence:** fgoodrum@arizona.edu

Summary

Liver X receptor (LXR) signaling broadly restricts virus replication; however, the mechanisms of restriction are poorly defined. Here, we demonstrate that the LXR-inducible cellular E3 ligase IDOL (inducible degrader of low-density lipoprotein receptor, LDLR) restricts replication of the beta-herpesvirus, human cytomegalovirus (HCMV), for the establishment of viral latency. IDOL is highly expressed in undifferentiated hematopoietic cells where HCMV establishes latency, but is sharply downregulated upon differentiation, a stimulus for reactivation. Importantly, IDOL restricts replication by driving the instability of a key viral determinant required for reactivation, the 33-kDa protein encoded by *UL136* (UL136p33). *UL136* encodes multiple proteins that differentially impact latency and reactivation. UL136p33 is targeted for rapid turnover by the proteasome and its stabilization by mutation of lysine residues to arginine results in a failure to quiet replication for latency. We show that IDOL interacts with and targets UL136p33 for turnover, but not the stabilized variant. While induction of IDOL prevents reactivation from latency, IDOL depletion increases viral gene expression in undifferentiated hematopoietic cells. This work establishes the UL136p33-IDOL interaction as a key regulator of the bistable switch between latency and reactivation. It further suggests a model whereby a key viral determinant of HCMV reactivation is regulated by a host E3 ligase and acts as a sensor at the tipping point between the decision to maintain the latent state or exit latency for reactivation.

Significance

Herpesviruses establish life-long latent infections, which pose an important risk for disease particularly in the immunocompromised. Our work is focused on the beta-herpesvirus, human cytomegalovirus (HCMV) that latently infects the majority of the population worldwide. Defining the mechanisms by which HCMV establish latency or reactivate from latency is important to controlling disease. Here, we demonstrate that the cellular inducible degrader of low-density lipoprotein receptor, IDOL, targets a HCMV determinant of reactivation for degradation. The instability of this determinant is important for the establishment of latency. This work defines a pivotal virus-host interaction that allows HCMV to sense changes in host biology to navigate decisions to establish latency or replicate.

Introduction

Viral latency, the ability of a virus to persist indefinitely in the infected host, is a hallmark of herpesviruses. Latency is defined as a non-replicative state punctuated by sporadic reactivation events where the virus replicates productively for transmission. Human cytomegalovirus (HCMV) is a beta-herpesvirus that establishes latent infection in hematopoietic progenitor cells (HPCs) and cells of the myeloid lineage (1). Reactivation of HCMV from latency in the immunocompromised can result in life-threatening disease and is a particularly important risk factor in the context of stem cell and solid organ transplantation. The molecular mechanisms by which HCMV senses changes in the host to make decisions to maintain latency or reactivate from latency is important in developing novel strategies to control viral reactivation and subsequent CMV disease.

78 Latency is a complex multifactorial phenomenon dependent on viral determinants, host
79 cell intrinsic, innate, and adaptive responses, as well as host cell signaling and chromatin
80 remodeling (2). Current paradigms hold that HCMV reactivation is tightly connected to
81 hematopoietic cell differentiation (3-7) or inflammatory signaling (3, 8-10). However, much
82 remains to be understood about the precise host contributions and key viral factors that
83 navigate the entry into or exit from latency. We and others have defined roles of *UL133-*
84 *138* gene locus encoded within the UL*b*' region of the HCMV genome for latency and
85 reactivation. *UL138* is required for latency and its protein functions by regulating cell
86 surface receptor trafficking and signaling (11-14), innate immune responses (15) and also
87 contributes to repression of viral gene expression (16). *UL135*, by contrast, is required for
88 reactivation from latency, functioning in part by opposing the function of *UL138* (17-19).
89 *UL136* is expressed as 5 protein isoforms that have differential effects on the
90 establishment of latency or reactivation. The largest, membrane-associated isoforms,
91 UL136p33 (UL136p33) and p26, are required for reactivation, whereas the small, soluble
92 isoforms are required for latency in both *in vitro* and *in vivo* experimental models (20, 21).
93 Importantly, UL136 proteins accumulate with delayed kinetics relative to UL135 and
94 UL138 and maximal accumulation of *UL136* gene products depend on the onset of viral
95 DNA synthesis and/or entry into late phase. Given its kinetics and dependence on viral
96 DNA synthesis for maximal expression, we postulate that UL136 may negotiate
97 checkpoints that function to maintain latency or commitment to reactivation from latency.
98 Identifying host pathways regulating these viral determinants is key to defining the
99 mechanistic basis by which HCMV senses and responds to changes in host biology to
100 maintain latency or reactivate.

101

102 The cellular environment the virus encounters upon infection undoubtedly plays important
103 roles in the establishment of latency with a host of restriction factors prepared to silence
104 the viral genome, as well as a transcriptional milieu that impacts viral gene expression.
105 As an example, we have shown that the cellular transcription factor early growth response
106 factor-1 (EGR-1) drives the expression of UL138 for the establishment of latency (19, 22).
107 As EGR-1 is required to maintain stemness in the bone marrow niche and is highly
108 expressed in undifferentiated hematopoietic cells (23), cells are primed to drive the
109 expression of UL138 for latency upon infection. However, HCMV also regulates EGR-1
110 expression through the differential trafficking and turnover of the host receptor tyrosine
111 kinase, epidermal growth factor receptor (EGFR) upstream of EGR-1 (11, 18, 19) and
112 through direct targeting by microRNAs that promote reactivation (22). Thus, HCMV has
113 evolved a multi-pronge strategy to manipulate and utilized host pathways to regulate its
114 gene expression, hardwiring infection into host signaling pathways. With regards to
115 reactivation, activation of the major immediate early (MIE) transcriptional unit, encoding
116 the major transactivators for viral replication, is highly dependent on host transcription
117 factors in myeloid cells (24). Host transcription factors CREB, FOXO3a and AP-1 are
118 downstream of major signaling pathways, including Src, PI3K/Akt, and MEK/ERK, and
119 are important for re-expression of MIE genes (25-27). Further, UL7 encodes a ligand that
120 binds the cellular Fms-like tyrosine kinase 3 receptor (Flt-3R) that when secreted upon
121 reactivation activates PI3K/AKT and MAPK signaling to prevent cell death and stimulate
122 differentiation for reactivation (28, 29). Through its co-evolution with the human host, the
123 biology of HCMV infection has become tightly intertwined with the biology its host, which

124 reflects the complex mechanisms the virus has evolved to “sense” and “respond” to
125 changes in the cellular environment to make “decisions" to maintain latency or reactivate
126 from latency.
127
128 Here we demonstrate that the largest isoform of UL136, UL136p33, is targeted for rapid
129 turnover relative to other UL136 protein isoforms and that its instability ($t_{1/2}$~1 h) is
130 important to the establishment of latency. We identified the LXR-inducible degrader of
131 low-density lipoprotein receptor (LDLR) IDOL (also known as myosin regulatory light
132 chain interacting protein or MYLIP), as the host E3 ligase that targets UL136p33 for
133 turnover. IDOL expression is induced by oxysterol activation of the liver X receptor (LXR)
134 (30) and is regulated through hematopoietic differentiation (31, 32). In addition to LDLR,
135 IDOL also targets VLDLR and ApoER-2 and, therefore, is an important homeostatic
136 regulator of intracellular cholesterol (30, 33-35). The targeting of UL136p33 by IDOL
137 suggests that the virus has evolved to be responsive to changes in cellular cholesterol in
138 its commitment to reactivation. A model emerges whereby high levels of IDOL maintains
139 low levels of UL136p33 for the establishment of latency, and the downregulation of IDOL
140 by differentiation results in the accumulation of UL136p33 to drive reactivation. Indeed,
141 induction of IDOL results in increased turnover of UL136p33 and prevents reactivation of
142 HCMV from latency, whereas depletion of IDOL increases viral gene expression in
143 hematopoietic cells. Our findings define UL133p33 is a key viral determinant of HCMV
144 reactivation that acts as a sensor at the tipping point between the decision to maintain the
145 latent state or exit latency for reactivation.
146

147 **Results**

148 **UL136p33 is unstable and is targeted for proteasomal degradation**

149 *UL136* is expressed as at least 5 co-terminal protein isoforms (Fig. 1A). These isoforms
150 are encoded by transcripts with unique 5' ends and have distinct roles in viral latency and
151 reactivation (20, 21). The largest of these isoforms is a 33-kDa protein (UL136p33) that
152 is required for replication in endothelial cells as well as reactivation from latency in CD34+
153 HPCs and in humanized mice (20). Conversely, the two small isoforms p23 and p19
154 suppress replication in endothelial cells and promote latency in CD34+ HPCs and
155 humanized mice (21). The diametric nature of the UL136 system presupposes additional
156 levels of control to coordinate and commit to one infection program over another, thereby
157 allowing for either optimal replication/reactivation or robust latency. The UL136 isoforms,
158 and particularly the full-length isoform UL136p33, are uniquely labile and sensitive to
159 mechanical lysis while being processed (21). Based on this, we hypothesized that the
160 concentration of some UL136 isoforms is regulated by increased proteolysis, and that the
161 instability of UL136p33 may be important to establishing or maintaining latency.

162

163 To explore the possibility that UL136 isoforms have different stabilities, we analyzed the
164 levels of UL136 isoforms in infected fibroblasts treated with cycloheximide (CHX) to halt
165 protein synthesis. Cycloheximide treatment resulted in a striking loss of UL136p33, p25,
166 and p23, but not p26 or p19 (Fig. 1B, left panel). These results indicated differential
167 stability whereby UL136p33, p25, and p23 may be subject to more rapid turnover, while
168 other UL136 isoforms are relatively stable. Proteasome inhibition robustly rescued
169 UL136p33, p25, and p23 isoforms (Fig. 1B, right panel). Inhibition of the lysosome with

170 NH_4Cl had no effect on rescue of any of the UL136 isoforms; however, inhibition of both
171 the lysosome and proteasome showed a somewhat additive effect. Together, these
172 results indicate that the rapid turnover of UL136p33, p25, and p23 is regulated by the
173 proteasome.
174
175 To establish the kinetics of isoform turnover, we analyzed the decay of UL136 isoforms
176 in fibroblasts infected with TB40/E-*UL136*$_{myc}$ and treated with CHX at peak UL136 isoform
177 expression (Fig 1C). UL136p33 decayed with a half-life of 1 h ($t_{1/2}$=1 h) and p25 exhibited
178 a $t_{1/2}$=3 h, while all other isoforms were stable over the 6 h time course (Fig 1D). The p23
179 isoform accumulates to very low levels making the decay of this protein is difficult to
180 determine. The rapid decay of UL136p33 relative to the other isoforms, as well as its
181 significance in HCMV reactivation prompted us to focus on determining the factor(s)
182 contributing to its instability.
183
184 **Lysine to arginine mutations stabilize UL136p33**
185 UL136 has four lysine (K) residues (denoted by red lines in Fig. 1A), three of which lie
186 upstream of the transmembrane domain (TMD) and are unique to the p33 isoform. To
187 determine if the turnover of UL136p33 was regulated by ubiquitin-mediated proteolysis,
188 we substituted all lysine residues for arginine (R) through site-directed mutagenesis in an
189 expression vector encoding UL136p33 to generate *UL136p33*$_{myc}$*ΔK→R*. The p33$_{\Delta K\rightarrow R}$
190 mutant had a $t_{1/2}$=5 h, compared to ~1 h for UL136p33 following CHX treatment (Fig. 2A).
191 This observation, together with the stabilization of UL136p33 by proteasomal inhibition
192 (Fig. 1B), suggests that UL136p33 turnover is regulated by ubiquitin-mediated

193 proteasomal decay. Further, the rapid turnover of exogenously expressed UL136p33 (Fig.
194 2A, left panel) indicates that UL136p33's degradation is not dependent on virus or virus-
195 induced factors.
196
197 To determine the importance of UL136p33 instability in infection, we introduced the lysine
198 to arginine mutations into the *UL136*$_{myc}$ gene within the bacterial artificial chromosome
199 clone of TB40/E (*UL136*$_{myc}$*ΔK→R*). We measured the relative rates of decay in fibroblasts
200 infected with either the parental *UL136*$_{\mathrm{myc}}$ or *UL136*$_{myc}$*ΔK→R* virus and treated with CHX
201 and found that p33$_{\Delta K \rightarrow R}$ was stabilized during infection relative to wild type UL136p33 (Fig.
202 2B). Interestingly, we stabilization of UL136p33 diminished levels of UL136p26 and p25
203 isoforms by mechanisms that have yet to be determined.
204
205 We then performed multistep growth curves on fibroblasts infected with *UL136*$_{myc}$ or
206 *UL136*$_{myc}$*ΔK→R* to analyze the impact of stabilizing UL136p33 on virus replication. No
207 change in the kinetics or yield of viral growth was observed during the productive infection
208 in fibroblasts when UL136p33 is stabilized relative to the WT infection (Fig. 2C). This was
209 not surprising since the UL136p33 isoform, while important for replication in endothelial
210 cells and CD34+ HPCs, is dispensable for replication in fibroblasts (20, 21). In summary,
211 UL136p33 instability is the result of lysine-dependent, proteasomal degradation and
212 mutating lysine residues to arginine in *UL136* stabilizes the protein with no effect on virus
213 replication in fibroblasts.
214

215 Since UL136p33 is required for reactivation from latency in CD34+ HPCs (20), we
216 hypothesized that the instability of UL136p33 allows for a tunable concentration gradient
217 where low levels are important for the establishment of latency and accumulation past a
218 threshold is important for reactivation. To test this hypothesis, we performed a latency
219 assay in primary human CD34+ HPCs infected with the parental *UL136*$_{\text{myc}}$ or
220 *UL136*$_{myc}$*ΔK→R* viruses. *UL136*$_{myc}$-infected CD34+ HPCs generated >2-fold frequencies
221 of infectious centers following reactivation compared to the pre-reactivation control (Fig.
222 2D). However, the pre- and post-reactivation frequencies of infectious centers were not
223 different in the *UL136*$_{myc}$*ΔK→R* infection and were almost two-fold above *UL136*$_{\text{myc}}$ pre-
224 reactivation. These results indicate that HCMV replication in CD34+ HPCs is not quieted
225 when UL136p33 is stabilized, and that this virus does not establish a latent infection. As
226 is the case with many viral proteins, UL136 isoforms, even with a myc epitope tag, are
227 not expressed to detectable levels in hematopoietic cells, and we have been unsuccessful
228 in generating antibodies to UL136. Nevertheless, given the requirement for UL136p33 for
229 reactivation and replication in CD34+ HPCs, the *UL136*$_{myc}$*ΔK→R* infection phenotype is
230 consistent with accumulation of UL136p33 beyond a threshold critical for commitment to
231 reactivation.
232

233 **The host E3 ligase IDOL targets UL136p33 for proteasomal degradation**

234 Ubiquitination of cargo by E3 ligases is an important step in targeting a protein for
235 proteasomal degradation (36, 37). Because UL136p33 is rapidly turned over by the
236 proteasome even in the absence of infection and lysine to arginine substitutions stabilized
237 UL136p33, we hypothesized that a host E3 ligase targets UL136p33 for turnover. We

238 identified UL136 interacting proteins by a yeast two-hybrid screen (Y2H) using the C-
239 terminal region of UL136 (amino acids 141-240) as bait. Intriguingly, we identified the host
240 E3 ligase IDOL (**i**nducible **d**egrader **o**f **l**ow-density lipoprotein receptor), also known as
241 MYLIP, as a candidate host interactor of UL136 (Supporting information, SI Table 1).
242 IDOL induces the degradation of the low-density lipoprotein receptor family members
243 LDLR, VLDLR, and ApoER-2 (34, 35). The degradation of these receptors is a
244 physiological response to increased cholesterol, which is modified to oxysterols that
245 activate the LXR transcription factor to induce *IDOL* expression (35, 38, 39).
246
247 To determine if IDOL targets UL136p33, we analyzed the ability of IDOL to interact with
248 and impact UL136p33 levels. We validated the interaction between IDOL and UL136p33
249 by immunoprecipitating (IP) UL136p33-IDOL complexes from cells transiently
250 overexpressing myc-tagged UL136p33 or HA-tagged IDOL. Transient overexpression is
251 necessary due to the lack of commercially available antibodies specific and sensitive
252 enough to detect or immunoprecipitate endogenous IDOL. Pulldown of $IDOL_{HA}$ or $p33_{myc}$
253 coprecipitated the alternant partner (Fig. 3A), confirming the interaction between
254 UL136p33 and IDOL. Further analysis indicated that co-expression of IDOL with
255 UL136p33 resulted in a ~60% reduction in UL136p33 levels compared to when UL136p33
256 was co-expressed with an empty vector (Fig. 3B top and quantified in Fig. 3C), consistent
257 with IDOL driving UL136p33 turnover. By contrast, $p33_{\Delta K \rightarrow R}$ levels were not affected by
258 IDOL co-expression (Fig. 3B bottom and quantified in Fig. 3C), in agreement with the
259 hypothesis that ubiquitination on lysine residues is required for UL136p33 turnover via

260 the proteasome. Taken together, IDOL functions as a host E3 ligase that targets
261 UL136p33 for proteasomal degradation.
262
263 We next induced endogenous IDOL expression with an LXR agonist GW3965 or LXR-
264 independent agonist HBX41-108 in cells transiently expressing UL136p33 or $p33_{\Delta K \rightarrow R}$.
265 Because endogenous IDOL cannot be detected by western blot using available
266 antibodies (33, 40, 41), the induction of IDOL was verified by the loss of its target ApoER-
267 2 (Fig. 3D). Induction of IDOL, by both GW3965 and HBX41-108 resulted in a reduction
268 of UL136p33 (Fig. 3D, top), but not $p33_{\Delta K \rightarrow R}$ (Fig. 3D, bottom). These results further
269 confirm that endogenous IDOL targets UL136p33 for ubiquitin-dependent degradation.
270
271 The Y2H bait was composed of the C-terminal region of UL136 spanning amino acids
272 141-240 downstream of the predicted transmembrane domain. These residues are
273 shared by all the UL136 isoforms (Fig. 1A). Further, our data indicated that p25 and p23
274 proteins are also labile following CHX treatment and these smaller isoforms could be
275 rescued, like UL136p33, by inhibiting the proteasome (Fig. 1B, right panel). The p25 and
276 p23 isoforms have a single lysine which is located downstream of the TMD in the full
277 length UL136 isoform (Fig. 1A). Transient co-expression of IDOL with either p25 or p23
278 did not lead to any notable turnover of these proteins (SI Fig. 1A-C). These data
279 collectively led us to conclude that IDOL specifically targets UL136p33 for turnover, and
280 it does not mediate the degradation of p25 and p23. The mechanism by which p25 and
281 p23 are turned over remains to be elucidated.
282

283 To further define the specificity of IDOL-mediated turnover of UL136p33, we co-
284 expressed UL136p33 with another E3 ligase, Cbl. Cbl targets tyrosine kinase receptors,
285 such as EGFR, for ubiquitination and subsequent degradation by the lysosome (42).
286 Levels of UL136p33 were unaffected by co-expression with Cbl (SI Fig. 1D-E), indicating
287 specificity of IDOL for proteasomal turnover of UL136p33.
288

289 **IDOL impacts UL136p33 protein levels in HCMV-infected primary fibroblasts**

290 In the context of a productive infection in fibroblasts, we found that infection with either
291 the parental *UL136*$_{myc}$ or *UL136*$_{myc}$*ΔK→R* induced *IDOL* transcripts by at least 5-fold
292 compared to mock-infection by reverse transcriptase, quantitative PCR (RT-qPCR), (SI
293 Fig. 2A). *IDOL* transcript upregulation was sustained over time during infection and
294 peaked at close to 10-fold by 3 dpi. No changes in *IDOL* transcript levels were detected
295 in mock controls over the same time-course. Because *IDOL* induction is a consequence
296 of increased cellular cholesterol, we measured cholesterol content in infected cells to
297 correlate it to the upregulation of *IDOL* transcripts. Using this approach, we noted that
298 HCMV increased cholesterol concentration by at least 29% from 1 dpi onward (SI Fig.
299 2B), consistent with previous findings on HCMV-modulation of lipid biosynthesis (43-48).
300 Taken together, infection in fibroblasts upregulates expression levels of IDOL transcripts,
301 which is correlated with increased intracellular cholesterol levels.
302

303 To address the effect of HCMV-mediated induction of IDOL on UL136p33 levels in a
304 productive infection, we again induced IDOL expression with the LXR agonist GW3965
305 or HBX41-108 in TB40/E-*UL136*$_{myc}$- or -*UL136*$_{myc}$ΔK→R-infected fibroblasts. IDOL

306 induction resulted in a 50% reduction in the levels of UL136p33 but did not significantly
307 affect $p33_{\Delta K \rightarrow R}$ levels (SI Fig. 2C and D). Diminished levels of smaller UL136 isoforms are
308 again apparent in the *UL136*$_{myc}$ΔK→R infection. We next disrupted *IDOL* expression in
309 fibroblasts to answer the question whether IDOL depletion would rescue UL136p33
310 turnover. CRISPR-mediated knockout (KO) of *IDOL* using guide RNAs to disrupt all the
311 isoforms of IDOL was validated by Sanger sequencing and increased ApoER-2 as a proxy
312 for *IDOL* KO (SI Fig. 2E). Further, CRISPR KO of *IDOL* had no effect on HDAC1, a
313 potential off-target hit when knocking out *IDOL*. In fibroblasts depleted of IDOL, UL136p33
314 levels increased at 2 and 3 dpi compared to luciferase KO controls, but did not affect
315 levels of $p33_{\Delta K \rightarrow R}$ (SI Fig. 2F and quantified in 2G). Further, IE2 levels were also
316 significantly increased in IDOL KO cells infected with *UL136*$_{myc}$, but not changed by IDOL
317 KO in the *UL136*$_{myc}$K→R infection (SI Fig. 2H). Together, these results indicate that IDOL
318 regulates UL136p33 concentration, which indirectly impacts IE expression in the context
319 of infection.
320

321 **IDOL restricts HCMV reactivation**

322 HCMV latency is studied in a variety of models. Due to limitations unique to each model,
323 there is no perfect model and, therefore, we explore latency questions using multiple
324 complementary models. To explore the role of IDOL in regulating UL136p33 levels in
325 latency and reactivation, we will use two models of HCMV: (1) THP-1 cell line model and
326 (2) CD34+ primary HPC model. In the THP-1 monocytic cell line model, cells are infected
327 in an undifferentiated state for the establishment of latency. Viral gene expression is
328 detected early (1 dpi) following infection, but is silenced as the virus establishes a latent-

329 like state (49). Re-expression of viral genes for reactivation can be stimulated by
330 differentiating the cells into macrophages with a phorbol ester, tetradecanoylphorbol
331 acetate (TPA) (50-55). This is a strong model for looking at transcriptional changes
332 associated with latency and reactivation; however, this model is limited in that THP-1 cells
333 do not robustly or consistently support viral genome synthesis or production of viral
334 progeny following TPA induction of reactivation. The gold-standard for HCMV latency is
335 the ability of the virus to establish and reactivate from latency in primary human CD34+
336 HPCs (56). The primary CD34+ HPC model supports viral genome synthesis and the
337 formation of infectious progeny in response to reactivaiton, the gold-standard for
338 reactivation. However, the model is limited by substantial donor-variability of primary
339 human cells, heterogeneity of the population, the availability of the cells in numbers to
340 provide sufficient starting material for some assays, and the ability to manipulate these
341 cells (e.g. gene knockdowns or overexpression) without affecting their differentiation,
342 which impacts HCMV infection. Further, because reactivation of HCMV from CD34+
343 HPCs occurs at low frequency (1 in ~9,000 cells), analysis of molecular events associated
344 with reactivation is challenging. The use of both models yields complementary insights
345 into the patterns of gene expression upon infection or reactivation (THP-1), genome
346 synthesis and virus production (CD34+ HPCs) to understand latency and reactivation.
347
348 Dynamic gene expression changes are associated with monocyte-to-macrophage
349 differentiation (31, 57, 58). Because IDOL is highly expressed in bone marrow (59), we
350 hypothesized that *IDOL* expression may be dictated by the differentiation state of the cell
351 and would regulate UL136 levels in a differentiation-dependent manner. Indeed, we found

352 that *IDOL* was highly expressed in undifferentiated THP-1 monocytes prior to infection,
353 but was sharply downregulated upon THP-1 cell differentiation (Fig. 4A). Further, while
354 no significant differences in *IDOL* expression were observed between uninfected cells
355 and a $UL136_{myc}$ infection, $UL136_{myc}\Delta K\rightarrow R$ infection significantly downregulated *IDOL*
356 expression in the undifferentiated, latent phase (Fig. 4A). This result suggests that
357 UL136p33 levels may feedback to impact IDOL expression in a cell type-dependent
358 manner.
359
360 To determine how IDOL impacts HCMV infection in hematopoietic cells, we knocked out
361 *IDOL* in THP-1 cells using CRISPR. The knockdown was validated using an ELISA assay
362 for the detection of IDOL protein (Fig. 4B); IDOL protein was reduced in undifferentiated
363 cells to levels induced by differentiation. Further, *IDOL* KO had no off-target effects on
364 HDAC1 (Fig. 4C). Given the challenges of detecting UL136 isoforms, particularly in
365 hematopoietic cells, we examined IE1, IE2 and UL135 gene expression as proxies for
366 determining the effect of *IDOL* KO on infection in THP-1 cells. UL135 and IE1/2 proteins
367 are detected early during infection in THP-1 cells but diminish as the virus establishes
368 latency between 3 and 5 dpi (Fig. 4D-E) (50). *IDOL* KO resulted in an increased initial
369 burst in the expression of IE1, IE2, and UL135 at 1 dpi relative to control *Luc* KO cells.
370 Notably, the major HCMV transactivator, IE2, was only detected in the IDOL KO condition.
371 The increased viral gene expression in the IDOL KO is consistent with increased viral
372 activity and UL136p33 levels. However, gene expression was still relatively quieted by 5
373 dpi, suggesting not unexpectedly that other viral or cellular factors are required for
374 progression of rectivation. However, as we have never identified a condition or mutant

375 virus that is not ultimately silenced in THP-1 cells, it may be that the program for restriction
376 and silencing in this model is robust as indicated by the inability of these cells to support
377 viral DNA synthesis and progeny formation even with TPA treatment. Importantly, *IDOL*
378 KO had no effect on IE1, IE2, or UL135 expression in *UL136*$_{myc}$*ΔK→R* infection (Fig. 4D-
379 E), consistent with a role for IDOL in regulating the establishment of latency by targeting
380 UL136p33 for turnover. In contrast to *UL136*$_{myc}$ infection, IE2 is detected in all conditions
381 of the *UL136*$_{myc}$K→R infection and is not increased further by IDOL KO. While a potent
382 transactivator, IE2 feeds back to negatively regulate the major immediate early promoter
383 and its own expression (60-63). The differences in IE2 expression in IDOL KO in *UL136*$_{myc}$
384 and *UL136*$_{myc}$K→R infection may reflect complexities in the regulation of IE gene
385 expression and the possible dysregulation and loss of middle UL136 isoforms in
386 *UL136*$_{myc}$K→R infection (Fig. 2). These results indicate that IDOL negatively regulates
387 viral gene expression for the establishment of latency in undifferentiated THP-1 cells,
388 consistent with its role in maintaining low levels of UL136p33 and the role of UL136p33
389 in driving HCMV replication in hematopoietic cells (64). Further, these data indicate that
390 UL136p33 may negatively regulate IDOL expression.
391
392 To further explore the importance of IDOL in latency, we turned to the primary CD34+
393 HPC experimental model. We purified (GFP+) CD34+ HPCs infected with TB40/E-
394 *UL136*$_{myc}$ or -*UL136*$_{myc}$K→R by fluorescent activated cell sorting and seeded the cells into
395 long-term bone marrow cultures. IDOL was induced at 5 dpi after the establishment of
396 latency by GW396 treatment. IDOL induction was validated by the increased IDOL
397 transcripts in GW3965-treated cells compared to DMSO-treated cells (Fig. 5A). At 10 dpi,

398 the culture was split and half the cells were seeded by limiting dilution into co-culture with
399 fibroblasts and cytokine-rich media to stimulate reactivation from latency. The other half
400 were mechanically lysed and lystates were seeded by limiting dilution onto fibroblast
401 monolayers to determine the virus present prior to reactivation (pre-reactivation). Relative
402 to the DMSO control, GW3965 treatment restricted *UL136*$_{myc}$ reactivation (Fig. 5B),
403 consistent with a requirement for accumulation of UL136p33 for reactivation. Strikingly,
404 reactivation of *UL136*$_{myc}$*ΔK→R* was not restricted by GW3965-induction of IDOL. Given
405 the limited availability of human CD34+ HPCs, data from two independent donors are
406 shown. These results indicate that IDOL restricts virus reactivation in a manner
407 dependent on its ability to turnover UL136p33. Taken together with the THP-1
408 experiments, these results support the hypothesis that UL136p33 stability is required for
409 reactivation from latency and that induction of IDOL at reactivation suppresses UL136p33
410 from accumulating to levels sufficient for reactivation (Fig. 6).
411

412 **Discussion**

413 Latent viruses require mechanisms to sense the cellular environment, filter noise and
414 respond to host cues to make solid decisions to maintain a quiescent latent state or to
415 reactivate replication (1). While the decision to enter or exit latency is often depicted as a
416 simple binary on/off switch, the reality is more likely that a number of thresholds must be
417 reached to clear checkpoints in the commitment to productive reactivation. Developing
418 strategies to control entry into or exit from CMV latency and ultimately control CMV
419 disease rests upon identifying the virus-host interactions that govern the decisions around
420 latency and reactivation. Here we demonstrate the existence of an unstable viral

421 determinant of reactivation, UL136p33. We demonstrate that its instability is dependent
422 upon a host E3 ligase, IDOL, which is regulated by hematopoietic differentiation. Our
423 results support a model whereby UL136p33 is maintained at low levels for the
424 establishment of latency because IDOL levels are high (Fig. 6). Upon differentiation, IDOL
425 levels fall, allowing UL136p33 levels to rise, which facilitates HCMV crossing at least one
426 threshold towards reactivation. UL136p33 accumulation is amplified and re-enforced by
427 the onset of viral DNA synthesis and entry into late phase (21) and high levels of
428 UL136p33 suppresses IDOL expression (Fig. 4A). These findings define novel virus-host
429 interactions that govern entry into and exit from latency. Moreover, these findings suggest
430 that by utilizing IDOL to regulate levels of a critical determinant for reactivation, the virus
431 evolved to hardwire this decision into LXR signaling and the the regulation of intracellular
432 cholesterol, which ultimately controls IDOL levels.
433
434 *IDOL* is transcriptionally upregulated by excess cholesterol derivatives (oxysterols) that
435 are sensed by LXR and in a cell type-dependent manner (35, 65-68). RNA sequencing to
436 classify the tissue-specific expression of genes across a representative set of all major
437 human organs and tissues revealed that IDOL is highly upregulated in the bone marrow,
438 where CD34+ HPCs and monocytes are generated (69). The level of IDOL expression in
439 the BM is only second to the placenta. High expression of IDOL in undifferentiated
440 progenitor cells suggests they are intolerant of high cholesterol levels. Consistent with
441 this, undifferentiated THP-1 monocytes express significantly higher levels of cholesterol
442 efflux genes, such as CES1, and express significantly lower levels of influx genes (70).
443 By contrast, THP-1 monocyte-derived macrophages upregulate cholesterol influx genes,

444 such as scavenger receptor A1 (SR-A1) and CD36 to become lipid-loaded macrophages
445 or foam cells. Further, statin treatment to lower cholesterol reduces CD34+ HPC
446 populations in the circulation and high cholesterol promotes CD34+ HPC proliferation,
447 myelopoiesis as well as monocyte and granulocytic differentiation (71-73). While carefully
448 designed studies are required to understand how statins specifically affect HCMV latency
449 and/or reactivation, these findings suggest the possibility that untreated
450 hypercholesterolemia might lead to increased hematopoietic differentiation and a higher
451 frequency of HCMV reactivation events, whereas statin treatments may restrict HCMV
452 reactivation and replication. Given the role demonstrated here for IDOL in the regulation
453 of cholesterol and UL136p33 expression, the high levels of IDOL expression make
454 progenitor cells an ideal environment for HCMV latency in which UL136p33 is suppressed
455 by rapid turnover.
456
457 HCMV infection remodels the cellular lipid metabolic landscape by upregulating *de novo*
458 cholesterol biosynthesis during a productive infection (44, 47, 48). It is, therefore,
459 expected that HCMV infection would induce IDOL expression. While IDOL and
460 cholesterol are induced by infection in fibroblasts (SI Fig. 2A-B), IDOL expression was
461 not induced by infection in hematopoietic cells. In fact, IDOL expression was
462 downregulated by *UL136*$_{myc}$K→R infection (Fig. 4A). While cholesterol increases in
463 macrophage cells, their higher tolerance to cholesterol than HPCs or monocytes (74-76)
464 may not necessarily correspond to higher levels of IDOL, as we have shown. Accordingly,
465 despite increase cholesterol in macrophages, IDOL levels are strikingly downregulated in
466 THP-1 cells induced to differentiate with TPA (Fig. 4A).

467

468

469 IDOL recognizes a conserved motif WxxKNxxSI/MxF within the cytoplasmic tail of its
470 targets (ApoER-2, LDLR and VLDLR), to mediate ubiquitination for lysosomal
471 degradation (30, 34, 35, 77). Canonical IDOL targets reside at the plasma membrane and
472 are typically internalized via the endocytosis and trafficked to the lysosome (77). By
473 contrast, UL136p33 is predominantly Golgi-associated (21), lacks a WxxKNxxSI/MxF
474 motif, and is degraded via the proteasome (Fig. 1B). Differences in localization and
475 trafficking pathways between natural IDOL targets and UL136p33 may differentially direct
476 the degradation pathway.

477

478 Activation of LXR in human foreskin fibroblasts with GW3965 prior to HCMV infection has
479 been shown to depress expression levels of viral proteins, such as IE2, pp28, pp65 and
480 gB (78). GW3965 treatment is also reported to induce IFN-γ (79), a cytokine which
481 directly inhibits IE1/2 mRNA expression (80). These findings might suggest that possibility
482 that the effects of LXR agonists on UL136p33 levels are due to a global repression of
483 viral gene expression. However, our results argue against this scenario. First, we
484 observed no effect on IE gene expression at 2 dpi in infected fibroblasts treated with
485 GW3965 or HBX41-108 (Fig. S1C), consistent with the attenuation of IFN-γ at later times
486 (81). Second, specific depletion of *IDOL* increases UL136p33, consistent with IDOL-
487 specific effects on UL136p33 levels. Nevertheless, to avoid this potential pitfall, cells were
488 treated with these agonists following the establishment of infection and IE gene
489 expression in our studies.

490

491

492

493 The LXR axis is important for the biology of other herpesviruses. A recent report
494 demonstrates that the alpha herpesvirus pseudorabies virus (PRV), etiologic agent of the
495 economically important Aujeszky's disease, has evolved to inhibit LXR at both
496 transcription and protein levels (82). Using an inverse LXR agonist SR9243, Wang and
497 colleagues showed that inhibiting LXR increased PRV replication, whereas 3 different
498 LXR agonists and the oxysterol 22R-hydroxycholesterol all inhibited PRV replication (82).
499 However, PRV can be rescued from the suppressive effects of an LXR agonist by
500 supplementing with cholesterol (82), consistent with a viral need for cholesterol to
501 replicate. LXR also inhibits the murine gamma herpesvirus MHV68 as it replicates better
502 in *LXR*$^{-/-}$ macrophages and, contrary to PRV, MHV68 infection increases LXRα (83).
503 Importantly, LXRα restricts reactivation of MHV86 in peritoneal cells, but not in
504 splenocytes (84). The cell type-dependent role of LXR signaling for reactivation suggests
505 the possibility that a LXR signaling might control a MHV68 determinant of reactivation in
506 peritoneal cells that is dispensable in splenocytes. Similarly, disruption of or stabilization
507 of UL136p33 did not impact replication in fibroblasts (Fig. 2C) (21), but did impact
508 replication in HPCs and endothelial cells (Fig. 2D) (20). Viral factors encoded by MHV68
509 and regulated by LXR signaling have yet to be determined.

510

511 In addition to herpesviruses, LXR signaling suppresses the replication of other viruses,
512 including Hepatitis C Virus (HCV) (85, 86), human immunodeficiency virus (HIV) (87-89),

513 and Newcastle disease virus (NDV) (90). Intriguingly, activation of LXR signaling
514 suppresses hepatitis C virus (HCV) replication in an IDOL-dependent manner. The
515 suppression of HCV is presumably due to the requirement of LDLR for an entry receptor
516 since once infection is established, IDOL induction does not seem to have an effect on
517 HCV replication (91). However, there are mixed reports on the requirement for LDLR for
518 HCV entry or its specific function in HCV replication (92-94).
519
520 While many host pathways are implicated in the regulation of herpesvirus latency, the
521 interplay between viral determinants and their regulation by host mechanisms to
522 terminate activity is less well appreciated, particularly for HCMV. The expression of HSV-
523 1 ICP0, a critical protein for reactivation and replication, is suppressed by the host
524 neuronal microRNA-138 to facilitate latency (95, 96). Moreover, ICP0 was recently shown
525 to be regulated by the host E3 ligase, TRIM23, which is in turn, countered by the HSV-1
526 late protein, $\gamma_1$34.5 (97). While speculative, TRIM23 may moderate ICP0 protein levels to
527 suppress reactivation, where $\gamma_1$34.5 ensures the commitment to replication by blocking
528 TRIM23-mediated turnover of ICP0. Further, the E3 ubiquitin ligase, MDM2, restricts
529 levels of the Kaposi's sarcoma-associated herpesvirus (KSHV) transactivator,
530 RTA/ORF50, acting as pro-viral factor for latency (98). RTA/ORF50 in turn induces
531 degradation of vFLIP through the host Itch E3 ubiquitin ligase to attenuate vFLIP-driven
532 NFκB signaling for reactivation (99, 100). Coopting and regulating host E3 ligases to
533 target viral proteins for latency allows infections to respond quickly to host cues (e.g., prior
534 to changes requiring transcription of genes and translation of proteins) for reactivation.
535 Further, it will be important to determine if UL136p33 feeds back to regulate *IDOL*

536 expression based on the observation that stabilization of UL136p33 represses *IDOL*
537 expression in undifferentiated THP-1 cells (Fig. 5A). It will be important to further define
538 the mechanisms by which UL136p33 interacts with host pathways to impact viral gene
539 expression and promote context-dependent replication and reactivation.
540
541 The evolution of viruses to depend on host factor-mediated turnover of critical viral
542 determinants is shared across highly divergent systems. Bacteriophages establish a
543 dormant lysogenic state to cope with their variable and unpredictable environment (101).
544 Bacteriophage λ lysogeny depends on the competition between repressors and activators
545 of gene expression that serve as a gatekeeper for the lytic pathways (102, 103). As a
546 primary example, competitive binding of the lysogeny determinant CI and the immediate
547 early gene Cro at regulatory operator elements puts CI-Cro at the heart of a bistable
548 switch controlling lysogenic-lytic decisions. Another determinant, CII, is expressed with
549 later kinetics and is also critical to the commitment to lysogeny (104, 105). CII promotes
550 expression of CI while it represses expression of the anti-terminator Q, that must
551 accumulate to a threshold to drive lytic gene expression. Critical effectors in
552 bacteriophage lysogeny, such as CI and CII, are susceptible to destruction by host
553 proteases that are induced in response to stresses, such as DNA damage (106, 107). As
554 such, the decision to establish lysogeny depends on the accumulation of lysogenic
555 effectors and is responsive to host determinants regulated by environmental cues.
556 Further, while CI is robust, the expression of CII, like UL136, is sensitive to genome copy
557 number or other fluctuations in the system, providing additional checkpoints in regulating
558 the decision.

559

560 With respect to the system emerging for HCMV, the *UL133-UL138* locus coordinates the
561 expression of multiple genes impacting infection fate decisions. While UL135 and UL138
562 are not known to directly regulate gene expression, their opposing impact on host
563 EGFR/PI3K signaling (11, 17, 19) has parallels to the Cro-CI bistable genetic switch.
564 Further, UL136p33 is expressed with later kinetics than the UL135/UL138 determinants,
565 and robust UL136p33 expression is dependent on crossing a threshold of commitment to
566 viral DNA synthesis (21). In addition, UL136p33 is remarkably unstable compared to other
567 *UL133-UL138* genes and other UL136 isoforms, and, as we have shown here, its
568 instability is dependent upon a host E3 ligase regulated by differentiation-linked changes
569 in IDOL expression. Although the UL136p33 protein is undetectable in THP-1 monocytes,
570 KO of *IDOL* increases expression of genes critical for replication (e.g., IEs and UL135).
571 While UL135 is critical for overcoming the repressive effects of UL138 for successful
572 reactivation, we assert that the subsequent accumulation of UL136p33 beyond a
573 threshold is also important for commitment to the replicative state (Fig. 6). It will be
574 important to understand the relationship between UL135 and UL136p33 in the
575 commitment to HCMV reactivation since as both are required for reactivation and how
576 other UL136 isoforms, for example the latency-promoting UL136p23/19 isoforms (20),
577 may contribute to the establishment of latency or counter the progression towards
578 reactivation to maintain a latent infection. This is a particularly intriguing question as the
579 stabilization of UL136p33 not only affects levels of IDOL mRNA, but also affects levels of
580 the middle UL136 isoforms (Fig. 2B). These findings indicate that the LXR-IDOL axis may
581 be a potential target for controlling HCMV reactivation clinically.

582

583 **Methods**

584 **Cells and viruses**

585 Human primary embryonic fibroblasts (MRC-5; ATCC) and human kidney embryonic
586 293T (HEK 293T; ATCC) cells were maintained in Dulbecco's Essential Media (DMEM).
587 The DMEM was supplemented with 10% fetal bovine serum (FBS), 10 mM HEPES, 1 mM
588 sodium pyruvate, 2 mM l-alanyl-glutamine, 0.1 mM nonessential amino acids, 100 U/ml
589 penicillin, and 100 µg/ml streptomycin. CD34+ hematopoietic progenitor cells (HPCs)
590 were isolated from de-identified medical waste following bone marrow isolations from
591 healthy donors for clinical procedures at the Banner-University Medical Center at the
592 University of Arizona (56). THP-1 cells were maintained in RPMI1640 (Gibco)
593 supplemented with 10% FBS, 1 mM sodium pyruvate, 0.1 mM β-mercapto-ethanol
594 (Sigma).

595

596 The wild type TB40E/05 strain expressing GFP as a marker for infection (108) was
597 engineered to fuse the myc epitope tag in frame at the 3' end of *UL136* ($UL136_{myc}$ virus)
598 using BAC recombineering as described previously (21). The $UL136_{myc}\Delta K \rightarrow R$ virus was
599 constructed following methods previously described (Caviness 2014). See SI for detailed
600 description of virus recombineering.

601

602 **CRISPR/CAS9-mediated knock out of *IDOL***

603 Guide RNAs (gRNAs) used to knock out IDOL were designed using online gRNA design
604 tools at atum.bio and synthego.com. Sequences of the gRNAs are shown in SI Table 2.

605 The gRNAs were cloned into lentiCRISPR v2 (109). Lentiviruses to deliver the gRNAs
606 were generated by co-transfecting the lentiCRISPR v2 constructs with pDMG.2 and
607 psPAX2 in HEK 293T cells. MRC-5 and THP-1 cells were transduced at a MOI of 3 and
608 10, respectively. Transduced cells were selected with 2 µg/ml puromycin for 2 days.
609 Validation of knock-out was done by blotting for ApoER-2, Sanger sequencing or
610 quantifying levels of IDOL by ELISA. The Synthego gRNA design algorithm
611 (synthego.com) indicates potential off-target genes for the gRNAs and we selected
612 *HDAC1* to evaluate potential off-target effects by western blot analyses.
613

614 **IDOL ELISA**

615 We used a sandwich ELISA assay (Cusabio) to quantify IDOL protein levels in THP-1
616 cells. Cells were washed in cold PBS and resuspended at 10^8 cells/mL followed by
617 freezing at -20 ^{o}C. Following 3 freeze-thaw cycles, IDOL was quantified according to the
618 manufacturer's protocol. Optical densities were determined using a Clariostar plate
619 reader (BMG Labtech) and sample values were interpolated from a standard curve in
620 GraphPad Prism v9.
621

622 **Cholesterol assay**

623 Fibroblasts were seeded at 3 x 10^5 cells per well in 6-well dishes and incubated overnight.
624 Infections were done at a MOI of 1 for 1 h and the inoculum was removed followed by
625 washing cells twice with PBS. Infected cells were incubated in serum-free media and 50
626 000 cells were harvested at appropriate time points. Samples were prepared using a
627 cholesterol Glo bioluminescent assay (Promega) according to the manufacturer's

instructions. Relative light units were measured using a Clariostar Plus plate reader (BMG Labtech) and sample values were extrapolated from a standard curve in GraphPad Prism v9.

Latency assays

Latency assays in CD34+ HPCs were carried out as described previously (56). IDOL expression was induced prior to reactivation by treatment with 1 μM GW3965. Infections for latency in THP-1 cells were done as described previously (50)

Please see SI for detailed description of materials and methods.

Acknowledgements

This study was supported by the National Institutes of Allergy and Infectious Diseases/ National Institutes of Health (NIAID/NIH) grants AI079059 and AI131598 to FG. We are grateful for the support of the Flow Cytometry and Human Immune Monitoring Shared Resource, supported through the Cancer Center Support Grant P30 CA023074 awarded to University of Arizona. We appreciate technical assistance from Lincoln Gay. We thank Drs. James Alwine (University of Pennsylvania), Lynn Enquist (Princeton University), Jean Wilson (University of Arizona), and John Purdy (University of Arizona) for critical discussions on this work.

References

1. F. Goodrum, "The complex biology of human cytomegalovirus latency and reactivation" in Advances in Virus Research, T. C. M. M. Kielian, M. J. Roossinck, Ed. (Academic Press, 2022), vol. 112.
2. F. Goodrum, W. Britt, E. S. Mocarski, "Cytomegalovirus" in Fields Virology: DNA Viruses, P. M. Howley, D. M. Knipe, J. L. Cohen, B. A. Damania, Eds. (Wolters Kluwer, 2022), vol. 2, chap. 12.

654 3. G. Hahn, R. Jores, E. S. Mocarski, Cytomegalovirus remains latent in a common precursor of
655 dendritic and myeloid cells. *Proc Natl Acad Sci U S A* **95**, 3937-3942 (1998).
656 4. C.-K. Min *et al.*, The Differentiation of Human Cytomegalovirus Infected-Monocytes Is Required
657 for Viral Replication. **10** (2020).
658 5. M. B. Reeves, P. A. MacAry, P. J. Lehner, J. G. P. Sissons, J. H. Sinclair, Latency, chromatin
659 remodeling, and reactivation of human cytomegalovirus in the dendritic cells of healthy carriers.
660 *Proceedings of the National Academy of Sciences of the United States of America* **102**, 4140 (2005).
661 6. M. B. Reeves, J. H. Sinclair, Circulating dendritic cells isolated from healthy seropositive donors
662 are sites of human cytomegalovirus reactivation in vivo. *J Virol* **87**, 10660-10667 (2013).
663 7. J. Taylor-Wiedeman, J. G. P. Sissons, L. K. Borysiewicz, J. H. Sinclair, Monocytes are a major site of
664 persistence of human cytomegalovirus in peripheral blood mononuclear cells. **72**, 2059-2064
665 (1991).
666 8. E. Forte *et al.*, Tumor Necrosis Factor Alpha Induces Reactivation of Human Cytomegalovirus
667 Independently of Myeloid Cell Differentiation following Posttranscriptional Establishment of
668 Latency. *mBio* **9**, e01560-01518 (2018).
669 9. C. Söderberg-Nauclér, K. N. Fish, J. A. Nelson, Reactivation of Latent Human Cytomegalovirus by
670 Allogeneic Stimulation of Blood Cells from Healthy Donors. *Cell* **91**, 119-126 (1997).
671 10. M. B. Reeves, T. Compton, Inhibition of inflammatory interleukin-6 activity via extracellular signal-
672 regulated kinase-mitogen-activated protein kinase signaling antagonizes human cytomegalovirus
673 reactivation from dendritic cells. *J Virol* **85**, 12750-12758 (2011).
674 11. J. Buehler *et al.*, Opposing Regulation of the EGF Receptor: A Molecular Switch Controlling
675 Cytomegalovirus Latency and Replication. *PLOS Pathogens* **12**, e1005655 (2016).
676 12. M. P. Weekes *et al.*, Latency-Associated Degradation of the MRP1 Drug Transporter During Latent
677 Human Cytomegalovirus Infection. *Science* **340**, 199 (2013).
678 13. V. T. K. Le, M. Trilling, H. Hengel, The Cytomegaloviral Protein pUL138 Acts as Potentiator of Tumor
679 Necrosis Factor (TNF) Receptor 1 Surface Density To Enhance ULb'-
680 Encoded Modulation of TNF-α Signaling. *Journal of Virology* **85**, 13260 (2011).
681 14. C. Montag *et al.*, The Latency-Associated UL138 Gene Product of Human Cytomegalovirus
682 Sensitizes Cells to Tumor Necrosis Factor Alpha (TNF-α) Signaling by Upregulating TNF-α Receptor
683 1 Cell Surface Expression. **85**, 11409-11421 (2011).
684 15. E. R. Albright, C. K. Mickelson, R. F. Kalejta, Human Cytomegalovirus UL138 Protein Inhibits the
685 STING Pathway and Reduces Interferon Beta mRNA Accumulation during Lytic and Latent
686 Infections. *mBio* **12**, e0226721-e0226721 (2021).
687 16. S. H. Lee, E. R. Albright, J.-H. Lee, D. Jacobs, R. F. Kalejta, Cellular defense against latent
688 colonization foiled by human cytomegalovirus UL138 protein. *Sci Adv* **1**, e1501164-e1501164
689 (2015).
690 17. M. Umashankar *et al.*, Antagonistic Determinants Controlling Replicative and Latent States of
691 Human Cytomegalovirus Infection. *Journal of Virology* **88**, 5987 (2014).
692 18. M. A. Rak *et al.*, Human Cytomegalovirus UL135 Interacts with Host Adaptor Proteins To Regulate
693 Epidermal Growth Factor Receptor and Reactivation from Latency. **92**, e00919-00918 (2018).
694 19. J. Buehler *et al.*, Host signaling and EGR1 transcriptional control of human cytomegalovirus
695 replication and latency. *PLOS Pathogens* **15**, e1008037 (2019).
696 20. K. Caviness *et al.*, Complex Interplay of the UL136 Isoforms Balances
697 Cytomegalovirus Replication and Latency. *mBio* **7**, e01986-01915 (2016).
698 21. K. Caviness, L. Cicchini, M. Rak, M. Umashankar, F. Goodrum, Complex expression of the UL136
699 gene of human cytomegalovirus results in multiple protein isoforms with unique roles in
700 replication. *J Virol* **88**, 14412-14425 (2014).

701 22. I. Mikell *et al.*, HCMV miR-US22 down-regulation of EGR-1 regulates CD34+ hematopoietic
702 progenitor cell proliferation and viral reactivation. *PLoS Pathog* **15**, e1007854 (2019).
703 23. I. M. Min *et al.*, The Transcription Factor EGR1 Controls Both the Proliferation and Localization of
704 Hematopoietic Stem Cells. *Cell Stem Cell* **2**, 380-391 (2008).
705 24. D. Collins-McMillen, J. Kamil, N. Moorman, F. Goodrum, Control of Immediate Early Gene
706 Expression for Human Cytomegalovirus Reactivation. *Frontiers in cellular and infection*
707 *microbiology* **10**, 476 (2020).
708 25. B. A. Krishna, A. B. Wass, C. M. O'Connor, Activator protein-1 transactivation of the major
709 immediate early locus is a determinant of cytomegalovirus reactivation from latency. *Proc Natl*
710 *Acad Sci U S A* **117**, 20860-20867 (2020).
711 26. A. E. Hale *et al.*, FOXO transcription factors activate alternative major immediate early promoters
712 to induce human cytomegalovirus reactivation. *Proc Natl Acad Sci U S A* **117**, 18764-18770 (2020).
713 27. V. G. Kew, J. Yuan, J. Meier, M. B. Reeves, Mitogen and stress activated kinases act co-operatively
714 with CREB during the induction of human cytomegalovirus immediate-early gene expression from
715 latency. *PLoS Pathog* **10**, e1004195 (2014).
716 28. L. B. Crawford *et al.*, Human Cytomegalovirus Encodes a Novel FLT3 Receptor Ligand Necessary
717 for Hematopoietic Cell Differentiation and Viral Reactivation. *MBio* **9** (2018).
718 29. M. H. Hancock *et al.*, Human Cytomegalovirus UL7, miR-US5-1, and miR-UL112-3p Inactivation of
719 FOXO3a Protects CD34(+) Hematopoietic Progenitor Cells from Apoptosis. *mSphere* **6** (2021).
720 30. E. Scotti *et al.*, Targeted disruption of the idol gene alters cellular regulation of the low-density
721 lipoprotein receptor by sterols and liver x receptor agonists. *Mol Cell Biol* **31**, 1885-1893 (2011).
722 31. R. G. de Bruin *et al.*, Quaking promotes monocyte differentiation into pro-atherogenic
723 macrophages by controlling pre-mRNA splicing and gene expression. *Nat Commun* **7**, 10846
724 (2016).
725 32. Y. Liu, M. Tingart, S. Lecouturier, J. Li, J. Eschweiler, Identification of co-expression network
726 correlated with different periods of adipogenic and osteogenic differentiation of BMSCs by
727 weighted gene co-expression network analysis (WGCNA). *BMC Genomics* **22**, 254 (2021).
728 33. E. Scotti *et al.*, IDOL stimulates clathrin-independent endocytosis and multivesicular body-
729 mediated lysosomal degradation of the low-density lipoprotein receptor. *Mol Cell Biol* **33**, 1503-
730 1514 (2013).
731 34. C. Hong *et al.*, The E3 ubiquitin ligase IDOL induces the degradation of the low density lipoprotein
732 receptor family members VLDLR and ApoER2. *J Biol Chem* **285**, 19720-19726 (2010).
733 35. N. Zelcer, C. Hong, R. Boyadjian, P. Tontonoz, LXR regulates cholesterol uptake through Idol-
734 dependent ubiquitination of the LDL receptor. *Science* **325**, 100-104 (2009).
735 36. M. H. Glickman, A. Ciechanover, The ubiquitin-proteasome proteolytic pathway: destruction for
736 the sake of construction. *Physiological reviews* **82**, 373-428 (2002).
737 37. C. M. Pickart, Back to the future with ubiquitin. *Cell* **116**, 181-190 (2004).
738 38. J. Zhang, Q. Liu, Cholesterol metabolism and homeostasis in the brain. *Protein Cell* **6**, 254-264
739 (2015).
740 39. L. Zhang, K. Reue, L. G. Fong, S. G. Young, P. Tontonoz, Feedback regulation of cholesterol uptake
741 by the LXR-IDOL-LDLR axis. *Arterioscler Thromb Vasc Biol* **32**, 2541-2546 (2012).
742 40. J. Gao *et al.*, The E3 ubiquitin ligase IDOL regulates synaptic ApoER2 levels and is important for
743 plasticity and learning. *Elife* **6**, e29178 (2017).
744 41. J. K. Nelson *et al.*, Deubiquitylase Inhibition Reveals Liver X Receptor-independent Transcriptional
745 Regulation of the E3 Ubiquitin Ligase IDOL and Lipoprotein Uptake. *J Biol Chem* **291**, 4813-4825
746 (2016).
747 42. Anonymous, Cytomegalovirus. *Am J Transplant* **4 Suppl 10**, 51-58 (2004).

748 43. Y. Du, G. Zhang, Z. Liu, Human cytomegalovirus infection and coronary heart disease: a systematic
749 review. *Virol J* **15**, 31-31 (2018).
750 44. N. Gudleski-O'Regan, T. M. Greco, I. M. Cristea, T. Shenk, Increased expression of LDL receptor-
751 related protein 1 during human cytomegalovirus infection reduces virion cholesterol and
752 infectivity. *Cell Host Microbe* **12**, 86-96 (2012).
753 45. Y. Xi, S. Harwood, L. M. Wise, J. G. Purdy, Human Cytomegalovirus pUL37x1 Is Important for
754 Remodeling of Host Lipid Metabolism. *J Virol* **93** (2019).
755 46. Y. Xi, L. Lindenmayer, I. Kline, J. von Einem, J. G. Purdy, Human Cytomegalovirus Uses a Host Stress
756 Response To Balance the Elongation of Saturated/Monounsaturated and Polyunsaturated Very-
757 Long-Chain Fatty Acids. *mBio* **12** (2021).
758 47. Y. Yu, T. G. Maguire, J. C. Alwine, Human cytomegalovirus infection induces adipocyte-like
759 lipogenesis through activation of sterol regulatory element binding protein 1. *J Virol* **86**, 2942-
760 2949 (2012).
761 48. Y. Yu, F. J. Pierciey, Jr., T. G. Maguire, J. C. Alwine, PKR-like endoplasmic reticulum kinase is
762 necessary for lipogenic activation during HCMV infection. *PLoS Pathog* **9**, e1003266 (2013).
763 49. D. Collins-McMillen *et al.*, Alternative promoters drive human cytomegalovirus reactivation from
764 latency. *Proc Natl Acad Sci U S A* **116**, 17492-17497 (2019).
765 50. D. Collins-McMillen *et al.*, Alternative promoters drive human cytomegalovirus reactivation from
766 latency. *Proceedings of the National Academy of Sciences* **116**, 17492 (2019).
767 51. M.-C. Arcangeletti *et al.*, Human cytomegalovirus reactivation from latency: validation of a
768 "switch" model in vitro. *Virol J* **13**, 179-179 (2016).
769 52. L.-F. Yee, P. L. Lin, M. F. Stinski, Ectopic expression of HCMV IE72 and IE86 proteins is sufficient to
770 induce early gene expression but not production of infectious virus in undifferentiated
771 promonocytic THP-1 cells. *Virology* **363**, 174-188 (2007).
772 53. B. G. Weinshenker, S. Wilton, G. P. Rice, Phorbol ester-induced differentiation permits productive
773 human cytomegalovirus infection in a monocytic cell line. *J Immunol* **140**, 1625-1631 (1988).
774 54. N. Wagenknecht *et al.*, Contribution of the Major ND10 Proteins PML, hDaxx and Sp100 to the
775 Regulation of Human Cytomegalovirus Latency and Lytic Replication in the Monocytic Cell Line
776 THP-1. *Viruses* **7**, 2884-2907 (2015).
777 55. C. H. Lee *et al.*, Factors affecting human cytomegalovirus gene expression in human monocyte cell
778 lines. *Mol Cells* **9**, 37-44 (1999).
779 56. M. Peppenelli, J. Buehler, F. Goodrum, Human Hematopoietic Long-Term Culture (hLTC) for
780 Human Cytomegalovirus Latency and Reactivation. *Methods Mol Biol* **2244**, 83-101 (2021).
781 57. R. N. Ramirez *et al.*, Dynamic Gene Regulatory Networks of Human Myeloid Differentiation. *Cell*
782 *systems* **4**, 416-429.e413 (2017).
783 58. F. O. Martinez, S. Gordon, M. Locati, A. Mantovani, Transcriptional Profiling of the Human
784 Monocyte-to-Macrophage Differentiation and Polarization: New Molecules and Patterns of Gene
785 Expression. *The Journal of Immunology* **177**, 7303 (2006).
786 59. B. Fagerberg, J. Gnarpe, H. Gnarpe, S. Agewall, J. Wikstrand, Chlamydia pneumoniae but not
787 cytomegalovirus antibodies are associated with future risk of stroke and cardiovascular disease:
788 a prospective study in middle-aged to elderly men with treated hypertension. *Stroke* **30**, 299-305
789 (1999).
790 60. M. C. Pizzorno, G. S. Hayward, The IE2 gene products of human cytomegalovirus specifically down-
791 regulate expression from the major immediate-early promoter through a target located near the
792 cap site. *J Virol* **64**, 6154-6165 (1990).
793 61. J. M. Cherrington, E. L. Khoury, E. S. Mocarski, Human cytomegalovirus ie2 negatively regulates
794 alpha gene expression via a short target sequence near the transcription start site. *J Virol* **65**, 887-
795 896 (1991).

796 62. B. Liu, T. W. Hermiston, M. F. Stinski, A cis-acting element in the major immediate early (IE)
797 promoter of human cytomegalovirus is required for negative regulation by IE2. *J Virol* **65**, 897-903
798 (1991).
799 63. M. P. Macias, M. F. Stinski, An in vitro system for human cytomegalovirus immediate early 2
800 protein (IE2)-mediated site-dependent repression of transcription and direct binding of IE2 to the
801 major immediate early promoter. *Proc Natl Acad Sci U S A* **90**, 707-711 (1993).
802 64. K. Caviness *et al.*, Complex Interplay of the UL136 Isoforms Balances Cytomegalovirus Replication
803 and Latency. *mBio* **7**, e01986 (2016).
804 65. S. D. Lee, P. Tontonoz, Liver X receptors at the intersection of lipid metabolism and atherogenesis.
805 *Atherosclerosis* **242**, 29-36 (2015).
806 66. B. A. Janowski *et al.*, Structural requirements of ligands for the oxysterol liver X receptors LXRalpha
807 and LXRbeta. *Proc Natl Acad Sci U S A* **96**, 266-271 (1999).
808 67. B. A. Janowski, P. J. Willy, T. R. Devi, J. R. Falck, D. J. Mangelsdorf, An oxysterol signalling pathway
809 mediated by the nuclear receptor LXRα. *Nature* **383**, 728-731 (1996).
810 68. D. J. Peet, B. A. Janowski, D. J. Mangelsdorf, The LXRs: a new class of oxysterol receptors. *Current*
811 *Opinion in Genetics & Development* **8**, 571-575 (1998).
812 69. L. Fagerberg *et al.*, Analysis of the human tissue-specific expression by genome-wide integration
813 of transcriptomics and antibody-based proteomics. *Molecular & cellular proteomics : MCP* **13**,
814 397-406 (2014).
815 70. I. Fernandez-Ruiz, P. Puchalska, C. A. Narasimhulu, B. Sengupta, S. Parthasarathy, Differential lipid
816 metabolism in monocytes and macrophages: influence of cholesterol loading[S]. *Journal of Lipid*
817 *Research* **57**, 574-586 (2016).
818 71. T. R. Cimato, B. A. Palka, J. K. Lang, R. F. Young, LDL Cholesterol Modulates Human CD34+ HSPCs
819 through Effects on Proliferation and the IL-17 G-CSF Axis. *PLOS ONE* **8**, e73861 (2013).
820 72. P. K. Morgan, L. Fang, G. I. Lancaster, A. J. Murphy, Hematopoiesis is regulated by cholesterol
821 efflux pathways and lipid rafts: connections with cardiovascular diseases: Thematic Review Series:
822 Biology of Lipid Rafts. *Journal of Lipid Research* **61**, 667-675 (2020).
823 73. O. Soehnlein, F. K. Swirski, Hypercholesterolemia links hematopoiesis with atherosclerosis. *Trends*
824 *in endocrinology and metabolism: TEM* **24**, 129-136 (2013).
825 74. J. M. Radley, S. Ellis, M. Palatsides, B. Williams, I. Bertoncello, Ultrastructure of primitive
826 hematopoietic stem cells isolated using probes of functional status. *Experimental hematology* **27**,
827 365-369 (1999).
828 75. S. Shariatmadar *et al.*, Electronic volume of CD34 positive cells from peripheral blood apheresis
829 samples. *Cytometry. Part B, Clinical cytometry* **74**, 182-188 (2008).
830 76. M. P. Vacanti, A. Roy, J. Cortiella, L. Bonassar, C. A. Vacanti, Identification and initial
831 characterization of spore-like cells in adult mammals. *Journal of cellular biochemistry* **80**, 455-460
832 (2001).
833 77. A. C. Calkin *et al.*, FERM-dependent E3 ligase recognition is a conserved mechanism for targeted
834 degradation of lipoprotein receptors. **108**, 20107-20112 (2011).
835 78. B. Liu *et al.*, Inhibition of Human Cytomegalovirus Particle Maturation by Activation of Liver X
836 Receptor. *Front Microbiol* **13**, 846386-846386 (2022).
837 79. Q. Wang *et al.*, Identification of interferon-γ as a new molecular target of liver X receptor.
838 *Biochemical Journal* **459**, 345-354 (2014).
839 80. B. Sainz, H. L. LaMarca, R. F. Garry, C. A. Morris, Synergistic inhibition of human cytomegalovirus
840 replication by interferon-alpha/beta and interferon-gamma. *Virol J* **2**, 14 (2005).
841 81. K. A. Kropp *et al.*, Reversible inhibition of murine cytomegalovirus replication by gamma
842 interferon (IFN-γ) in primary macrophages involves a primed type I IFN-signaling subnetwork for

843 full establishment of an immediate-early antiviral state. *Journal of virology* **85**, 10286-10299
844 (2011).
845 82. Y. Wang *et al.*, Pseudorabies Virus Inhibits Expression of Liver X Receptors to Assist Viral Infection.
846 *Viruses* **14**, 514 (2022).
847 83. P. T. Lange, C. Schorl, D. Sahoo, V. L. Tarakanova, Liver X Receptors Suppress Activity of Cholesterol
848 and Fatty Acid Synthesis Pathways To Oppose Gammaherpesvirus Replication. *mBio* **9**, e01115-
849 01118 (2018).
850 84. P. T. Lange, C. N. Jondle, E. J. Darrah, K. E. Johnson, V. L. Tarakanova, LXR Alpha Restricts
851 Gammaherpesvirus Reactivation from Latently Infected Peritoneal Cells. *Journal of virology* **93**,
852 e02071-02018 (2019).
853 85. J. Zeng *et al.*, Liver X receptors agonists impede hepatitis C virus infection in an Idol-dependent
854 manner. *Antiviral Res* **95**, 245-256 (2012).
855 86. S. Bocchetta *et al.*, Up-regulation of the ATP-binding cassette transporter A1 inhibits hepatitis C
856 virus infection. *PLoS One* **9**, e92140 (2014).
857 87. H. Jiang *et al.*, Retinoic acid and liver X receptor agonist synergistically inhibit HIV infection in CD4+
858 T cells by up-regulating ABCA1-mediated cholesterol efflux. *Lipids Health Dis* **11**, 69 (2012).
859 88. L. Dubrovsky *et al.*, Liver X receptor agonist inhibits HIV-1 replication and prevents HIV-induced
860 reduction of plasma HDL in humanized mouse model of HIV infection. *Biochem Biophys Res*
861 *Commun* **419**, 95-98 (2012).
862 89. T. M. Hanley, G. A. Viglianti, Nuclear receptor signaling inhibits HIV-1 replication in macrophages
863 through multiple trans-repression mechanisms. *J Virol* **85**, 10834-10850 (2011).
864 90. X. X. Sheng *et al.*, The LXR ligand GW3965 inhibits Newcastle disease virus infection by affecting
865 cholesterol homeostasis. *Arch Virol* **161**, 2491-2501 (2016).
866 91. J. Zeng *et al.*, Liver X receptors agonists impede hepatitis C virus infection in an Idol-dependent
867 manner. *Antiviral Research* **95**, 245-256 (2012).
868 92. G. H. Syed *et al.*, Hepatitis C virus stimulates low-density lipoprotein receptor expression to
869 facilitate viral propagation. *Journal of virology* **88**, 2519-2529 (2014).
870 93. A. Albecka *et al.*, Role of low-density lipoprotein receptor in the hepatitis C virus life cycle.
871 *Hepatology (Baltimore, Md.)* **55**, 998-1007 (2012).
872 94. S. Molina *et al.*, The low-density lipoprotein receptor plays a role in the infection of primary
873 human hepatocytes by hepatitis C virus. *Journal of hepatology* **46**, 411-419 (2007).
874 95. B. Sun *et al.*, Regulation of host and virus genes by neuronal miR-138 favours herpes simplex virus
875 1 latency. *Nature microbiology* **6**, 682-696 (2021).
876 96. D. Pan *et al.*, A neuron-specific host microRNA targets herpes simplex virus-1 ICP0 expression and
877 promotes latency. *Cell Host Microbe* **15**, 446-456 (2014).
878 97. X. Liu *et al.*, Herpesvirus-mediated stabilization of ICP0 expression neutralizes restriction by
879 TRIM23. *Proc Natl Acad Sci U S A* **118** (2021).
880 98. T. H. Chang *et al.*, Regulation of the Abundance of Kaposi's Sarcoma-Associated Herpesvirus
881 ORF50 Protein by Oncoprotein MDM2. *PLoS Pathog* **12**, e1005918 (2016).
882 99. J. C. Chmura *et al.*, The Itch ubiquitin ligase is required for KSHV RTA induced vFLIP degradation.
883 *Virology* **501**, 119-126 (2017).
884 100. E. S. Ehrlich, J. C. Chmura, J. C. Smith, N. N. Kalu, G. S. Hayward, KSHV RTA abolishes NFkappaB
885 responsive gene expression during lytic reactivation by targeting vFLIP for degradation via the
886 proteasome. *PLoS One* **9**, e91359 (2014).
887 101. S. Gandon, Why Be Temperate: Lessons from Bacteriophage λ. *Trends in Microbiology* **24**, 356-
888 365 (2016).

889 102. S. Atsumi, J. W. Little, Role of the lytic repressor in prophage induction of phage lambda as
890 analyzed by a module-replacement approach. *Proceedings of the National Academy of Sciences*
891 *of the United States of America* **103**, 4558-4563 (2006).
892 103. R. A. Schubert, I. B. Dodd, J. B. Egan, K. E. Shearwin, Cro's role in the CI Cro bistable switch is critical
893 for {lambda}'s transition from lysogeny to lytic development. *Genes Dev* **21**, 2461-2472 (2007).
894 104. M. G. Cortes, J. T. Trinh, L. Zeng, G. Balazsi, Late-Arriving Signals Contribute Less to Cell-Fate
895 Decisions. *Biophys J* **113**, 2110-2120 (2017).
896 105. O. Kobiler, A. Rokney, A. B. Oppenheim, Phage lambda CIII: a protease inhibitor regulating the
897 lysis-lysogeny decision. *PLoS One* **2**, e363 (2007).
898 106. J. W. Little, D. P. Shepley, D. W. J. T. E. j. Wert, Robustness of a gene regulatory circuit. **18**, 4299-
899 4307 (1999).
900 107. J. D. Hernandez-Doria, V. Sperandio, Bacteriophage Transcription Factor Cro Regulates Virulence
901 Gene Expression in Enterohemorrhagic Escherichia coli. *Cell Host Microbe* **23**, 607-617.e606
902 (2018).
903 108. M. Umashankar *et al.*, A Novel Human Cytomegalovirus Locus Modulates Cell Type-Specific
904 Outcomes of Infection. *PLOS Pathogens* **7**, e1002444 (2011).
905 109. N. E. Sanjana, O. Shalem, F. Zhang, Improved vectors and genome-wide libraries for CRISPR
906 screening. *Nat Methods* **11**, 783-784 (2014).

907

908

909 **Figure legends**

910

911 **Figure 1. UL136p33 isoform is rapidly turned over by the proteasome.** (A) Schematic
912 depiction of the *UL133-UL138* polycistronic gene locus and UL136 protein isoforms. A C-
913 terminal myc tag is used to detect UL136 isoforms. Red lines represent lysine residues,
914 and the black box shows the putative transmembrane domain. (B-D) Fibroblasts were
915 infected with TB40/E-$UL136_{myc}$ virus at a MOI of 1. (B) At 48 hpi, cells were treated with
916 50 µg/ml cycloheximide (CHX) for 6 h. Alternatively, mock- or TB40/E-infected cells were
917 treated with CHX in the context of proteasomal (MG132) or lysosomal (NH_4Cl) inhibition
918 (right panel). $UL136_{myc}$ protein isoforms or tubulin as a loading control were detected by
919 immunoblotting using by a monoclonal α-myc antibody or tubulin, respectively (left panel).
920 (C) Cells were untreated or treated with CHX at 48 hpi and UL136 decay was analyzed

921 over a 6-hour time course by immunoblotting. (D) Relative quantification of UL136
922 isoforms normalized to tubulin. HPT, hours post treatment
923
924 **Figure 2. Stabilizing UL136p33 results in virus that fails to establish latency.** (A)
925 Fibroblasts were transduced with lentiviruses engineered to express $p33_{myc}$ or $p33_{K\rightarrow R}$
926 and protein decay was analyzed by immunoblotting following CHX treatment. (B)
927 Fibroblasts were infected with TB40/E-*UL136*$_{myc}$ or -*UL136*$_{myc}$*ΔK→R* viruses (MOI =1)
928 and treated with CHX at 48 hpi or left untreated. Protein decay was analyzed as described
929 in Figure 1C. (C) Fibroblasts were infected at a MOI of 0.02 and samples collected for
930 $TCID_{50}$ at indicated times. All data points are an average of 3 biological replicates and
931 error bars represent standard deviation. (D) CD34+ HPCs were infected with *UL136*$_{myc}$
932 or *UL136*$_{myc}$*ΔK→R* viruses (MOI=2). Infected cells were purified by FACS at 1 dpi seeded
933 into long term culture. At 10 days, half of the culture was reactivated by seeding intact
934 cells by limiting dilution into co-culture with fibroblasts in a cytokine-rich media to promote
935 myeloid differentiation (reactivation). The other half of the culture was mechanically lysed
936 and seeded onto fibroblasts as the pre-reactivation control. The frequency of infectious
937 centers was determined for each sample by extreme limiting dilution. (C-D) The data
938 represents replicates with cells from 3 independent donors. The means were compared
939 with two-way analysis of variance (ANOVA) with a Tukey post hoc test and the were no
940 significant differences. **, $p<0.01$; ***, $p<0.001$.
941
942 **Figure 3. The host E3 ligase IDOL specifically targets UL136p33 for turnover.** (A)
943 HEK cells were transiently transfected with plasmids expressing UL136p33, IDOL, empty
944 vector, or the indicated combinations. UL136p33 or IDOL was immunoprecipitated from

945 protein lysates using α-myc or α-HA magnetic beads. Protein was detected by
946 immunoblotting using the antibodies indicated. Lysates were blotted as a control for
947 expression and GAPDH used as a loading control. (B) HEK cells were transiently
948 transfected with plasmids expressing $p33_{\Delta K \rightarrow R}$, IDOL, or empty vector. Proteins were
949 detected by immunoblotting using α-myc or α-HA monoclonal antibodies. (C) Protein
950 densities of UL136p33 (from panel A) or $p33_{\Delta K \rightarrow R}$ (from panel B) relative to their loading
951 control. (D) HEK cells were transiently transfected to express UL136p33 or $p33_{\Delta K \rightarrow R.}$ IDOL
952 was induced 48 hours later with 2 μM of LXR-agonists, GW3965 or HBX41-108, or vehicle
953 (DMSO) for 6 h. Detection of ApoER-2 was used as a proxy for validating the induction
954 of IDOL. $p33_{myc}$, $p33_{K \rightarrow R}$, and tubulin as a loading control were detected by
955 immunoblotting using α-myc or α-tubulin. All data points represent the mean of at least 3
956 independent replicates and the means were compared by two-way ANOVA with a Tukey
957 post hoc test. Error bars represent standard deviation. ns, $p>0.05$. ****, $p<0.0001$.
958

959 **Figure 4. IDOL impacts viral protein expression in a THP-1 cell latency model.** (A)
960 Total RNA was extracted from mock-, *UL136$_{myc}$*- or *UL136$_{myc}$ΔK→R*-infected THP-1 cells
961 at indicated time points. At 5 dpi, cells were treated with TPA to induce differentiation or
962 the vehicle control (DMSO). cDNA was synthesized from the RNA and qPCR was used
963 to determine the relative expression levels of *IDOL* transcripts compared to the low copy
964 cellular housekeeping gene *H6PD* using the ΔΔCT method. (B) Validation of *IDOL* KO in
965 undifferentiated THP-1 cells was confirmed by ELISA. Where indicated, cells were treated
966 with TPA as a positive control for the loss of IDOL. (C) Immunoblot of HDAC1 in *Luc*
967 control or *IDOL* KO THP-1 cells to rule out off-target CRISPR/CAS9 effects. (D) *IDOL* or

968 *Luc* KO THP-1 cells were infected with TB40/E-*UL136*$_{myc}$ (top panel) or -*UL136*$_{myc}$*K→R*
969 (bottom panel) at a MOI of 2 and cell lysates were collected at indicated time points. IE1/2
970 and UL135 accumulation was evaluated by immunoblotting protein lysates over a time
971 course using a monoclonal α-IE1/2 and polyclonal α-UL135. (E) IE1/2 and UL135 were
972 quantified, and levels normalized to Tubulin and levels present at 1 dpi in the Luc KO
973 control. All data points are representative of the mean 3 independent replicates and error
974 bars represent standard deviation. The means were compared by two-way ANOVA with
975 a Tukey post hoc test. ns, $p>0.05$; *, $p<0.05$; **, $p<0.01$; ****, $p<0.0001$.
976
977 **Figure 5. Induction of IDOL in CD34+ HPCs inhibits reactivation.** (A) CD34+ HPCs
978 were mock- or TB40/E-infected at a MOI of 2. At 1 dpi, cells were treated with 1 μM
979 GW3965 for 6 h and total RNA isolated for qPCR to measure *IDOL* transcript levels
980 relative to *H6PD*. The data points represent the mean from 3 independent experiments.
981 The means were analyzed by two-way ANOVA with a Tukey post-hoc test. ***$p<0.001$;
982 ****, $p<0.0001$. (B) CD34+ HPCs were infected at a MOI of 2. At 24 hpi, infected CD34+
983 cells were isolated by FACS and seeded into long term culture. GW3965 (1 μM) at 24 hpi.
984 At 10 days, half of the culture was reactivated by seeding intact cells by limiting dilution
985 into co-culture with fibroblasts in a cytokine-rich media to promote myeloid differentiation
986 (reactivation). The other half of the culture was mechanically lysed and seeded onto
987 fibroblasts as the pre-reactivation control. The frequency of infectious centers was
988 determined for each sample by ELDA. The data points represent replicates from 2
989 independent donors and the range is indicated by squares (pre-reactivation) and dots
990 (post-reactivation).

991

992 **Figure 6. Model for differentiation-dependent IDOL regulation to control UL136p33**
993 **levels.** Progenitor cells are relatively small and are intolerant of high cholesterol, which
994 they control by upregulating IDOL. We propose that high levels of IDOL maintain low
995 levels of UL136p33 for the establishment of latency. Upon cell differentiation, cells
996 downregulate IDOL, which would result in a corresponding increase in UL136p33 levels
997 to drive infection towards reactivation. UL136p33 levels are further increased upon the
998 commitment to viral DNA synthesis. Stabilization of UL136p33 results in corresponding
999 downregulation of IDOL mRNAs, suggesting feedback to suppress of IDOL gene
1000 expression. This work implicates IDOL as a host factor that fine-tunes levels of UL136p33
1001 to control decisions to enter and exit latency. These findings further indicate a key role for
1002 cholesterol homeostasis as a determinant of HCMV reactivation, whereby UL136p33 acts
1003 as a sensor at the tipping point between the decision to maintain the latent state or exit
1004 latency for reactivation. Cholesterol represented by beige droplets. Figure made with
1005 Biorender.com.

1006

1007 **Figure 1**

1008

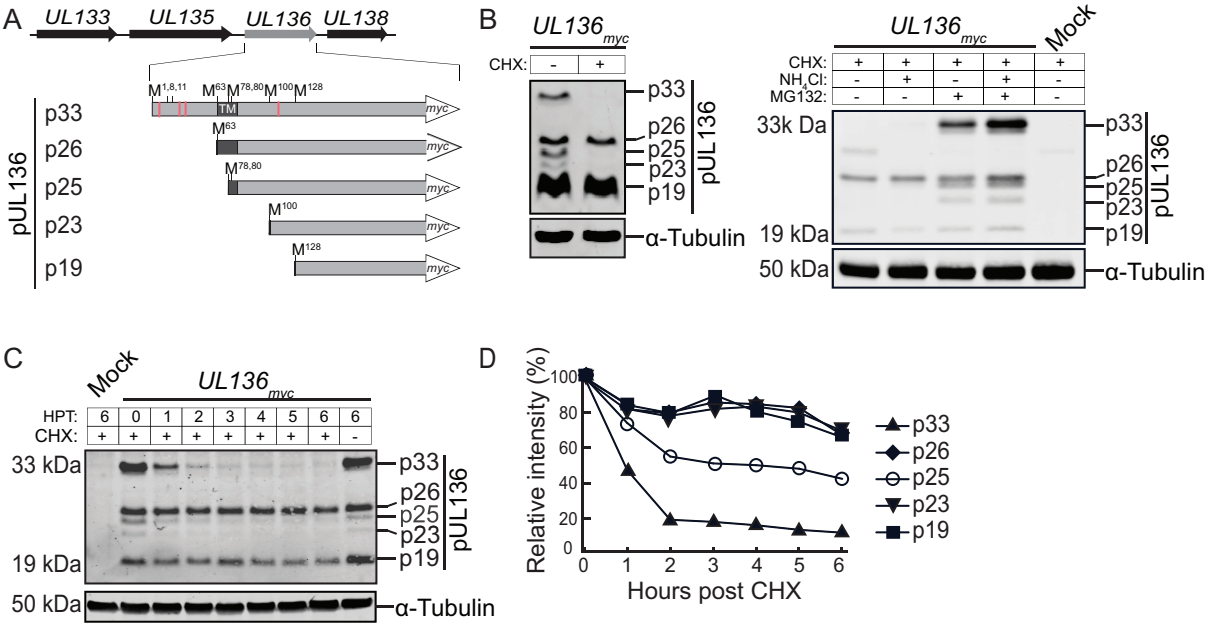

1009

1010 **Figure 2**

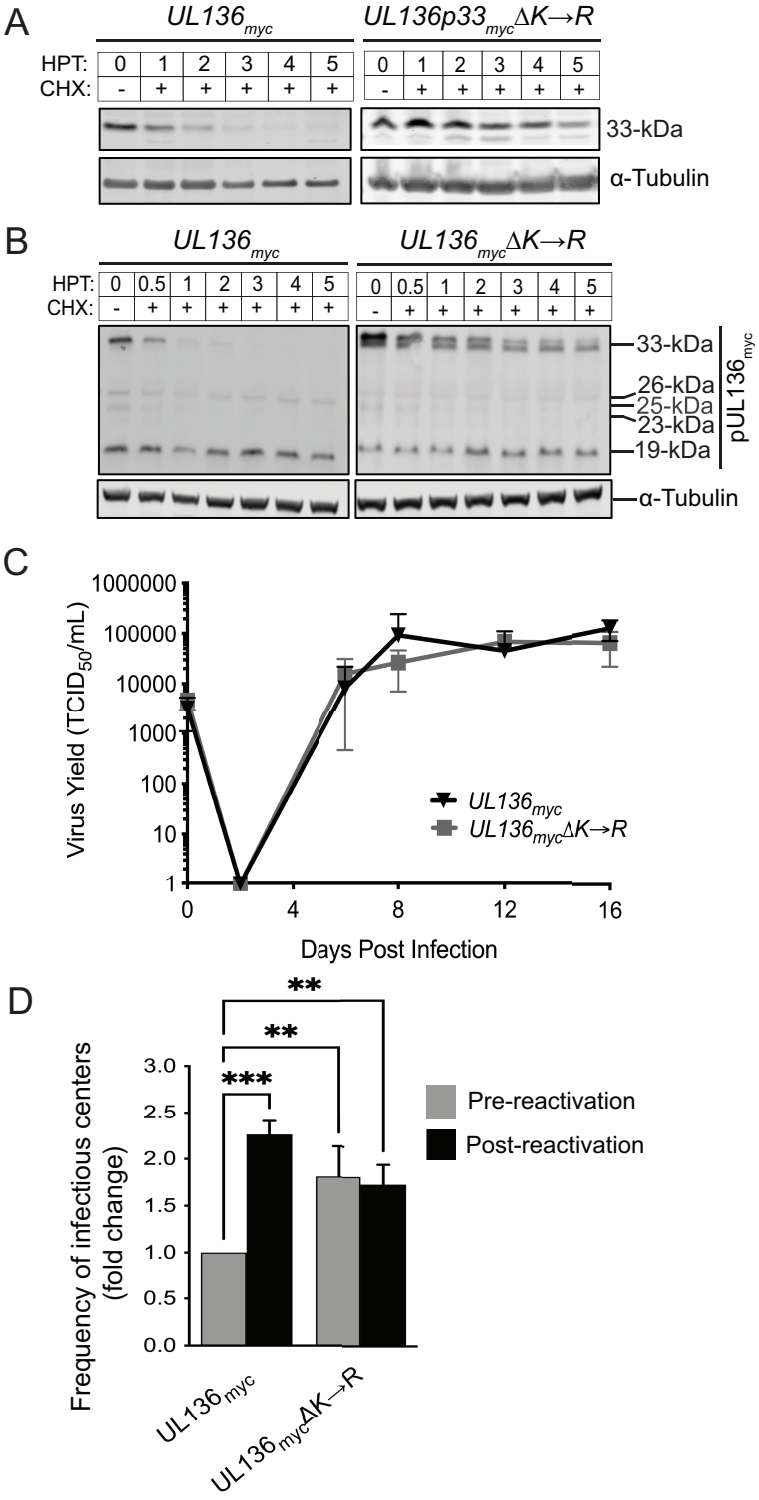

1011

1012

1013 **Figure 3**

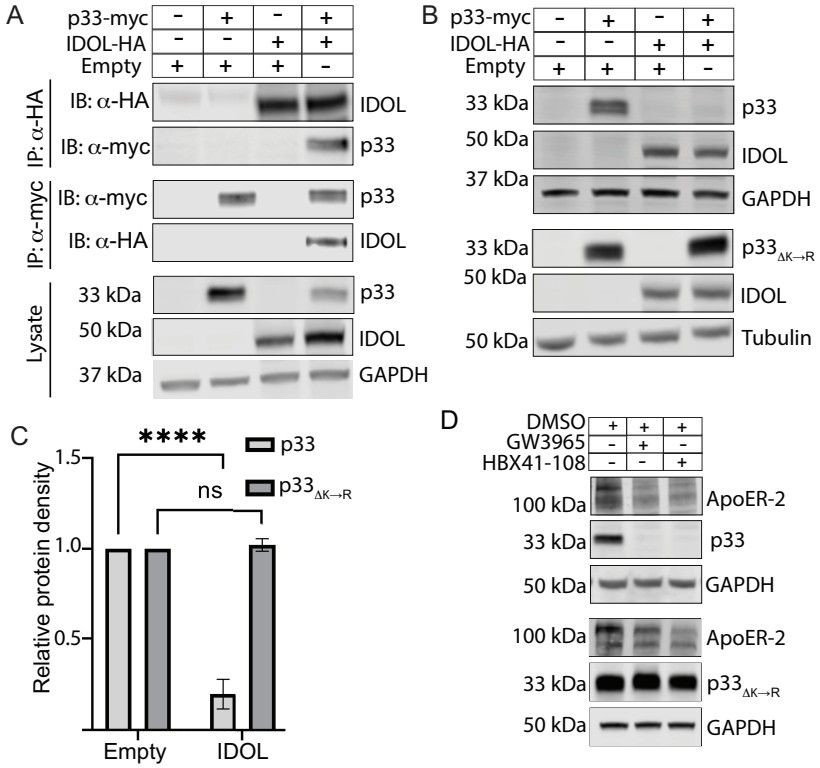

1014

1015

1016 **Figure 4**

1017

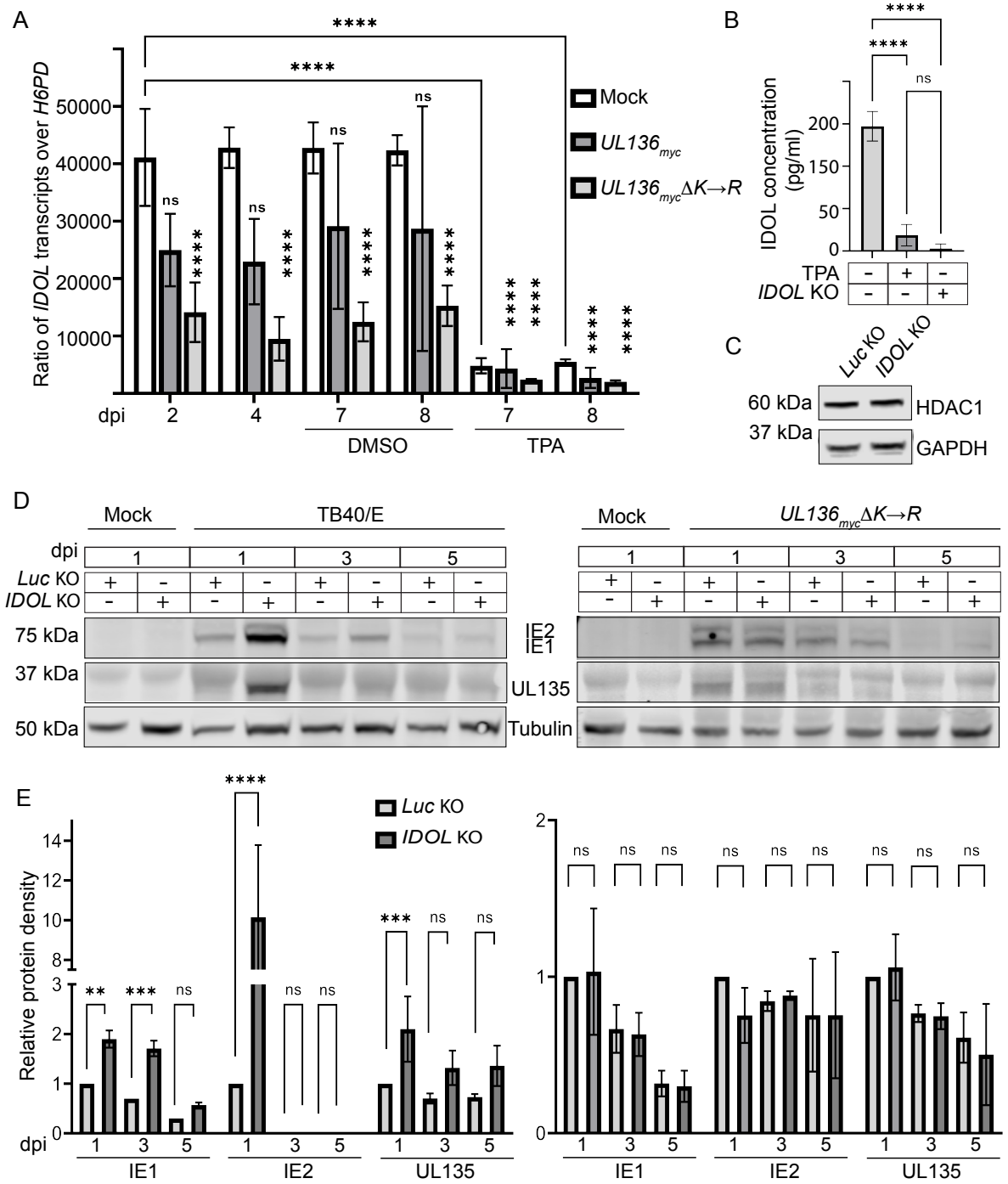

1018

1019 **Figure 5**

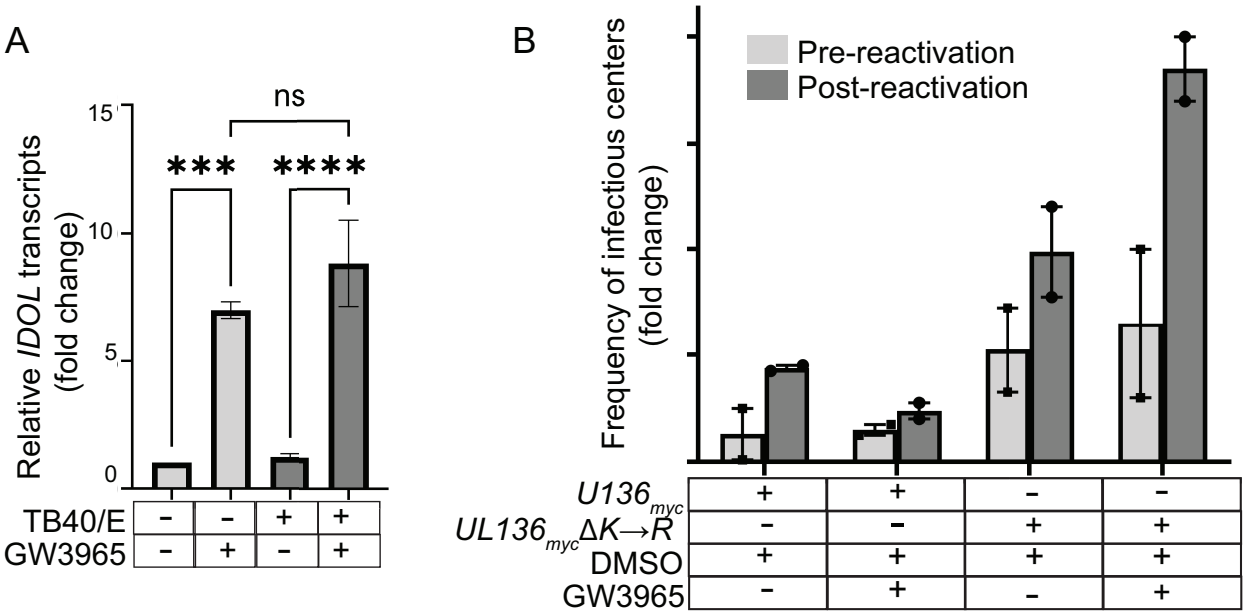

1020

1021 **Figure 6**

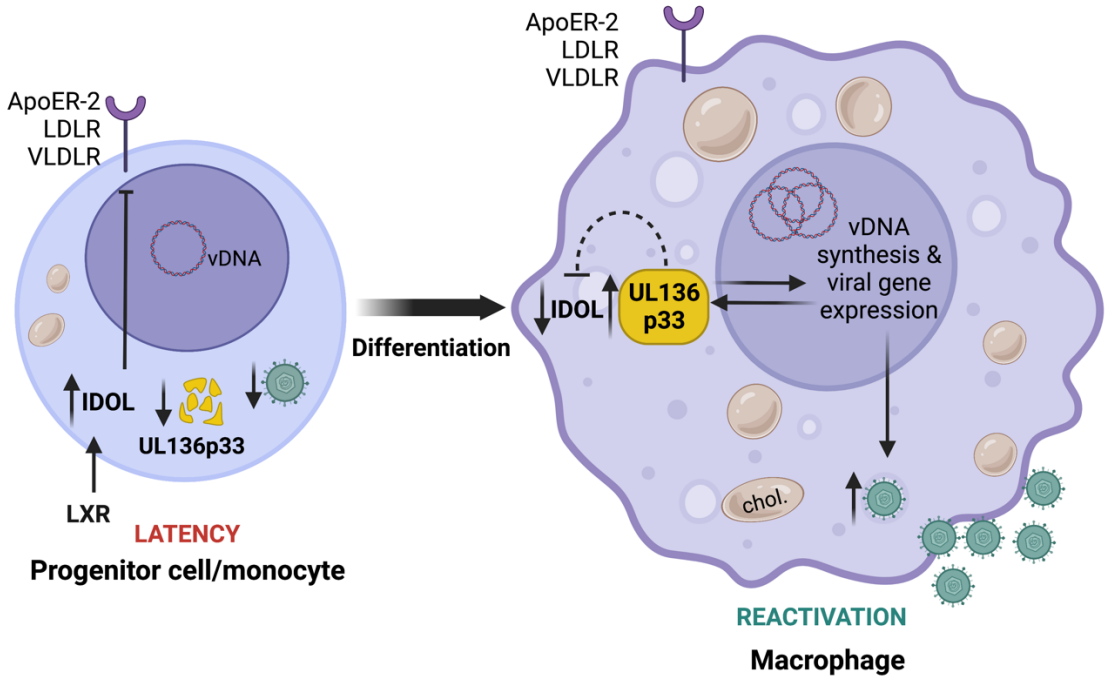

1022

1023 **SUPPORTING INFORMATION**

1024

1025 **SI Figure 1**

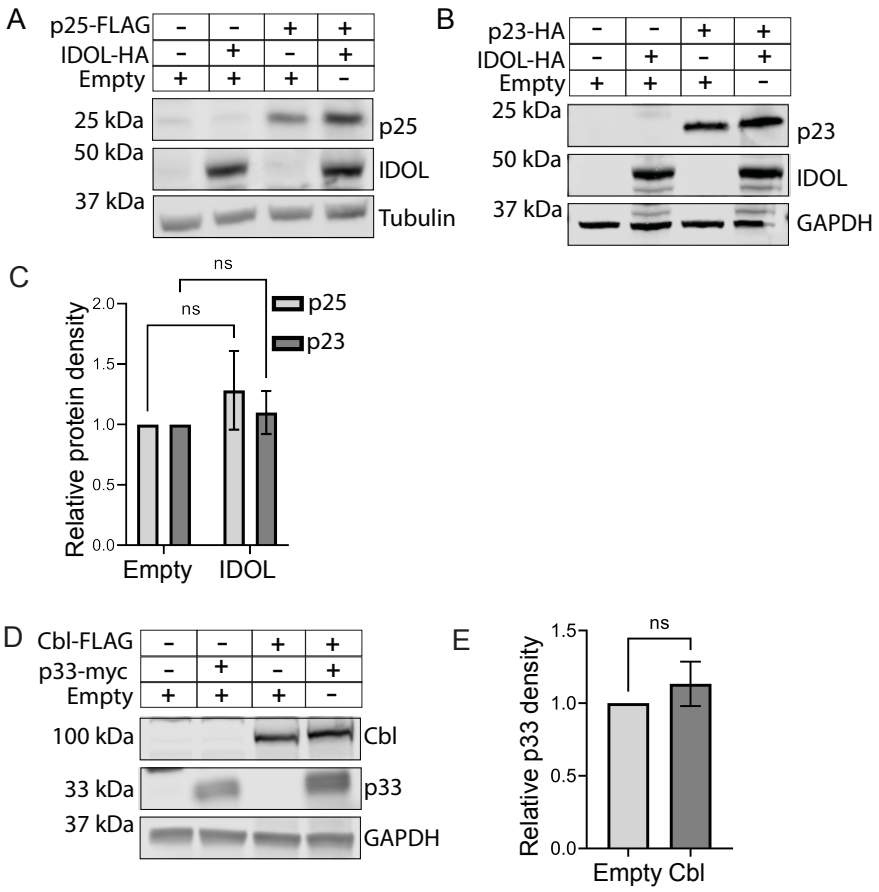

1026

1027

1028

1029 **SI Figure 1. IDOL specifically targets the UL136p33 isoform.** (A-C) HEK 293T cells were
1030 transfected with plasmids expressing (A) IDOL, p25 or empty vector or (B) IDOL, p23 or empty
1031 vector. Proteins detected by immunoblotting using antibodies to FLAG or HA to detect the
1032 indicated proteins. Tubulin or GAPDH were used as loading controls for normalization. (C)
1033 Relative p25 or p23 densities. (D) HEK 293T cells were co-transfected with plasmids expressing
1034 UL136p33, the E3 ligase Cbl or empty vector. Proteins were detected by immunoblotting using
1035 antibodies to the myc epitope tag or cbl. (E) Relative UL136p33 densities were measured and
1036 quantified. All data points represent the mean of at least 3 independent replicates and the means
1037 were compared by two-way ANOVA with a Tukey post hoc test. Error bars represent standard
1038 deviation. ns, non-significant

1039

1040

1041 **SI Figure 2**

1042

1043

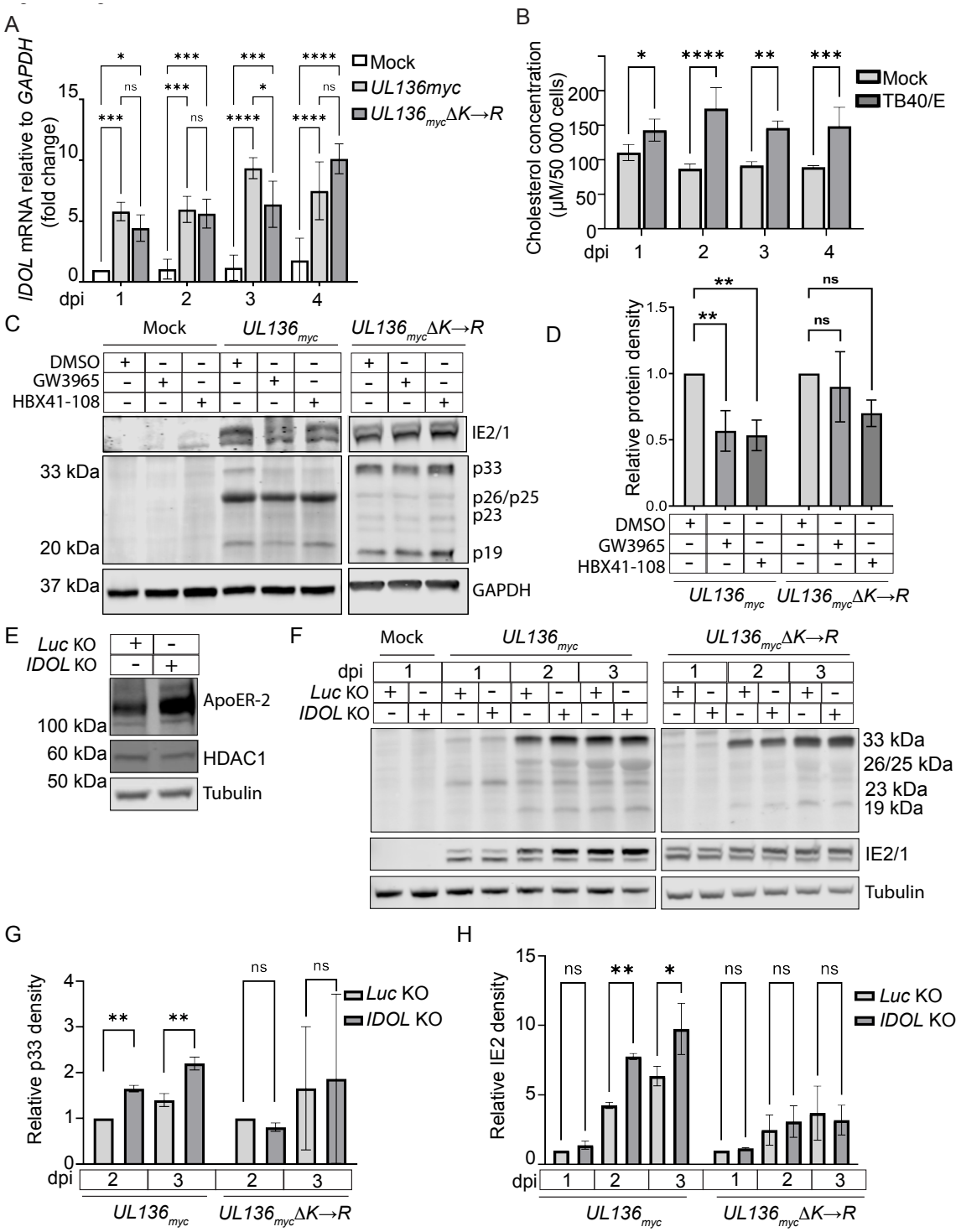

1044

1045

1046 **SI Figure 2. IDOL expression in HCMV-infected fibroblasts impacts UL136p33 stability.** (A)
1047 Fibroblasts were mock-infected or infected with *UL136*$_{myc}$ or *UL136*$_{myc}$*K→R* viruses at a MOI of 1
1048 and total RNA extracted at indicated time points. RT-qPCR was used to quantify relative *IDOL*
1049 transcripts using the ΔΔCT method. *IDOL* transcripts were normalized to GAPDH and compared
1050 to expression levels in mock samples at 1 dpi. (B) Fibroblasts were infected with TB40/E at a MOI
1051 of 1 followed by incubation in serum-free media. Cholesterol concentrations were measured and
1052 compared to mock-infected cells at 1 dpi. (C) Fibroblasts were mock-infected or infected with
1053 *UL136*$_{myc}$ or *UL136*$_{myc}$*ΔK→R* viruses at a MOI of 1. At 2 dpi, IDOL expression was induced by
1054 treatment with 2 μM GW3965 or HBX41-108 for 6 h followed by western blot evaluation of
1055 UL136p33 levels (left). Relative UL136p33 levels are quantified in (D). (E) *IDOL* KO cell lysates
1056 were analyzed by western blot to evaluate ApoER-2 expression levels compared to a *Luc* KO
1057 control. To evaluate CRISPR/CAS9 off-target effects we measured HDAC1 in *Luc* or *IDOL* KO
1058 cell lysates. (F) *UL136*$_{myc}$ or *UL136*$_{myc}$*ΔK→R* viruses were used to infect either *Luc* or *IDOL* KO
1059 cells at a MOI of 1. Cell lysates were collected at indicated times and evaluated for UL136p33
1060 expression levels that are quantified in (G). (H) Relative quantification of IE2 protein densities in
1061 *Luc* or *IDOL* KO fibroblasts. Quantitative data points represent the mean of 3 independent
1062 replicates and error bars represent standard deviation. Data points are means of 3 independent
1063 replicates and error bars represent standard deviation. Differences in the means were compared
1064 using two-way ANOVA with a Tukey post hoc test. ns, $p>0.05$; *, $p<0.05$; **, $p<0.01$; ***, $p<0.001$;
1065 ****, $p<0.0001$.

1066

1067

1068

1069

1070

1071

1072

1073

1074

1075

1076

1077

1078

1079 **SI Table 1. Candidate UL136 interactors from Y2H screen**

Name		Known Functions	Accession Number
MYLIP	Myosin regulatory light chain interacting protein	E3 Ubiquitin Ligase that mediates ubiquitination and degradation of myosin regulatory light chain (MRLC)	XM_005249032.2
PIK3R4	Phosphoinositide-3-kinase, regulatory subunit 4	Also called VPS15; serine-threonine protein kinase found at the cytoplasmic face of late Golgi and may regulate membrane trafficking in the late endocytic pathway	NM_014202.2
AP3B1	Adapter-related protein complex 3, beta 1 subunit	Subunit of non-clathrin- and clathrin-associated adaptor protein complex 3 that functions in transmembrane protein sorting to lysosome or lysosomal-related organelles.	NM_003664.4
CTSL2	Cathespin L2	Member of peptidase C1 family; lysosomal cysteine proteinase	NM_001333.3
TNFR-SF11B	Tumor necrosis factor receptor superfamily, member 11B	TNFR superfamily member; may act as a decoy receptor for TRAIL thereby protecting against apoptosis	NM_002546.3
CTNNAL1	Catenin (cadherin-associated protein), alpha-like 1	May modulate Rho pathway and act as anchor for PKA	XM_011519161.1
MARK3	MAP/microtubule affinity-regulating kinase 3	Activated by phosphorylation, then phosphorylates MAP2, MAP4, and CDC25	XM_006720146.2
ZFP42	Zinc finger protein 42	Also called Rex1; marker of pluripotency, regulation is critical to maintaining pluripotent state in ES cells and may be involved in transcriptional regulation	NM_001304358.1

MYLIP	Myosin regulatory light chain interacting protein	E3 Ubiquitin Ligase that mediates ubiqutination and degradation of myosin regulatory light chain (MRLC)	XM_005249032.2
SCEL	Sciellin	Localizes to periphery of cells; is a precursor of the cornified envelope of terminally differentiated keratinocytes	XM_011535281.1
CHCHD4	Coiled-coil-helix-coiled-coil-helix domain containing 4	Mitochondrial chaperone to catalyze disulfide bonds. Required for the import and folding of small cysteine containing proteins into the mitochondrial intermembrane space	NM_001098502.1
ADSL	Adenylosuccinate lyase	De novo synthesis of purines; catalyzes reactions in synthesis of AMP	XM_011529976.1
BTF3	Basic transcription factor 3	Forms stable complex with RNA polymerase II; required for transcription initiation	NM_001037637.1
DARS	Aspartyl-tRNA synthetase	Part of multienzyme complex of aminoacyl-tRNA synthetases; charges its cognate tRNA with aspartate	NM_001349.3
TERF2IP	Telomeric repeat binding factor 2, interacting protein	Part of a complex involved in telomere length regulation	NM_018975.3
CCDC15	Coiled-coil domain containing 15	?	NM_025004.2
CPORF43	Chromosome 9, open reading frame 43	?	NM_152786.2

1082 **SI Table 2. gRNAs used to KO *IDOL* and *luciferase (Luc)* gene (from *Photinus pyralis*)**

Gene	Position	Forward sequence	Reverse sequence
IDOL	16,145,148	CACCG**GCGCCGTGATGATG CAGUAU**[a]	AAACAUACUGCAUCAUCACGG CGCC
IDOL	16,143,526	CACCG**CCUUUUUGUUUUAG GUGUGC**	AAACGUUUCUCAGGUUUAGCC AUAC
IDOL	16,143,613	CACCG**UAUGGCUAAACCUG AGAAAC**	AAACGUUUCUCAGGUUUAGCC AUAC
Luc	1355	CACCG**ACAACUUUACCGAC CGCGCC**	AAAC**GGCGCGGUCGGUAAAGU UGU**

1083 [a]gRNA sequence is in bold text, and the preceding sequence was used to facilitate cloning onto
1084 the lentiCRISPR v2 vector.

1085

1086 **SI Table 3. Antibodies used in this study**

Antibodies		
Rabbit monoclonal anti-ApoER-2	Abcam	Cat#ab108208
Rabbit polyclonal anti-FLAG tag	Sigma-Aldrich	Cat#F7425
Rabbit monoclonal anti-GAPDH (clone D16H11)	Cell Signaling Technology	Cat#5174
Rabbit polyclonal anti-HA tag	Sigma-Aldrich	Cat#H6908
Mouse HDAC1 (clone 10E2)	Santa Cruz Biotech	Cat#sc-81598
IE1/2 (3H4)	Princeton University/Dr. Tom Shenk	N/A
Rabbit monoclonal anti-Myc tag (clone 71D10)	Cell Signaling Technology	Cat#2278
Tubulin (clone DM1A)		Cat#T6199
UL135	Open Biosystems	Custom antibody
Goat anti-mouse secondary antibody (IR Dye 680)	LI-COR Biosciences	Cat#926-68070

Goat anti-rabbit secondary antibody (IR Dye 800)	LI-COR Biosciences	Cat#926-32211

1087

1088

1089

1090

1091 **Materials and Methods**

1092

1093 **Yeast two-hybrid screen**

1094 A yeast screen for human cellular interacting proteins of pUL136 was performed using the
1095 Matchmaker Gold Yeast Two-Hybrid System (Clontech) and the Mate and Plate Universal Human
1096 Library (Clontech). This yeast two-hybrid universal library was constructed from human cDNA that
1097 has been normalized to remove high copy number cDNAs (overrepresented transcripts) to
1098 facilitate the discovery of low copy number novel protein-protein interactions. All protocols were
1099 carried out according to the manufacturer's guidelines. Yeast dual transformation and yeast
1100 mating was performed according to established protocols from Clontech. Yeast prey vectors were
1101 isolated from Y187 yeast and subsequently transformed into DH10B *E. coli*. After selection for *E*
1102 *coli* containing yeast prey vectors, the plasmids were isolated and sequenced to identify
1103 interacting partners.

1104

1105 **Bacterial Artificial Chromosome Recombineering**

1106 For generation of $UL136_{\mathrm{myc}}\Delta$K→R, $UL136_{myc}\Delta K\rightarrow R$ pGEM-T Easy construct was created by site-
1107 directed Phusion mutagenesis according to the manufacturer's instruction (New England Biolabs).
1108 Inverse PCR was used to mutagenize lysines 4, 20, 25, and 113 to arginine using the primers: 5'-
1109 GACGTTGGAAATAGATGGCGGCGTCGAAGGCCCTGAGTCGC-3' (forward);
1110 CAAGTCCCACGTCATTTCTGGCATCTCCACGCCCCTGACTGACAT-3' (reverse) for the first 3
1111 lysine residues in the N-terminal region and 4th lysine was mutagenized to arginine with the
1112 forward primer 5'-ACGAGCGGCAGAGAAGCAGACGGC-3', and reverse primer
1113 GGTGCCGACGGCACCTCTCAGGATAATG-3'. Following verification by Sanger sequencing, a
1114 region of the *UL136K-Rmyc* pGEM-T Easy was PCR amplified from bp 854 of UL135
1115 [UL135(bp854)] to UL138 (bp139). This PCR product was gel purified and recombined with a
1116 ΔUL136<GalK> BAC as previously described (21). BAC integrity was tested by enzyme digest
1117 fragment analysis and sequencing of the UL133/8 viral genomic region. All BAC genomes were
1118 maintained in Escherichia coli SW102, and viral stocks were propagated by transfecting 15 to 20
1119 µg of each BAC genome, along with 2 µg of a plasmid encoding UL82 (pp71), into 5 × 106 MRC-
1120 5 fibroblasts and subsequently purified and stored as previously described (21).

1121

1122 **Immunoblot analyses**

1123 Cells were washed twice in PBS (Gibco) and lifted from cell culture vessels with 0.25X trypsin
1124 (Gibco). Cells were washed in cold PBS, pelleted at 1000 xg for 2 minutes followed by storage at

-80 °C before lysis in RIPA buffer. Total protein was quantified using a BCA assay and 50 µg of each sample was prepared for loading onto 12% precast PAGE gels (GenScript). Wet transfers were performed onto 0.45 uM pore-sized PVDF membranes (Immobilon). Blocking was achieved by 5% skimmed milk in 1X TBST, or 5% BSA in 1X TBST. Primary and secondary antibodies used for western blot analyses are indicated in SI Table 3.

RT-qPCR assays

Cells were washed twice in cold PBS and lysed in 400 µl of RNA/DNA lysis buffer (Zymo Research). Total cellular RNA was extracted according to the manufacturer's protocol. cDNA was synthesized from 1 µg of DNAse-treated RNA using the Vilo cDNA synthesis kit (Invitrogen). qPCR reactions were prepared with *IDOL* TaqMan assay (ID Hs00982312_m1; ThermoFisher Scientific), Platinum™ Quantitative PCR SuperMix-UDG w/ROX (ThermoFisher Scientific) and 50 ng cDNA. qPCR reactions were run in a QuantStudio 3 real time PCR machine (Applied Biosystems). Gene expression was normalized to GAPDH (Hs01922876_u1) or H6PD (Hs00188728_m1) and the ΔΔCT method was used to calculate relative gene expression levels (110, 111).

Co-immunoprecipitation

Cells were washed twice with PBS and trypsinized. The PBS-washed cell pellet was lysed on ice for 30 minutes in a lysis buffer made of 100 mM Tris/HCl (pH 7.4), 100 mM NaCl, 50 mM NaFl, and 0.5% NP-40. The complete protease inhibitor cocktail (Roche) was added to the lysis buffer according to manufacturer recommendations. Lysates were clarified by centrifugation at 3000 x g for 5 minutes at 4 °C. A milligram of the lysate was incubated with Pierce anti-myc or anti-HA magnetic beads for 1 h at 4 °C. The beads were washed 3 times and protein eluted according to manufacturer's protocol.

References for Supporting Information

1. F. Goodrum, "The complex biology of human cytomegalovirus latency and reactivation" in Advances in Virus Research, T. C. M. M. Kielian, M. J. Roossinck, Ed. (Academic Press, 2022), vol. 112.
2. F. Goodrum, W. Britt, E. S. Mocarski, "Cytomegalovirus" in Fields Virology: DNA Viruses, P. M. Howley, D. M. Knipe, J. L. Cohen, B. A. Damania, Eds. (Wolters Kluwer, 2022), vol. 2, chap. 12.
3. G. Hahn, R. Jores, E. S. Mocarski, Cytomegalovirus remains latent in a common precursor of dendritic and myeloid cells. *Proc Natl Acad Sci U S A* **95**, 3937-3942 (1998).
4. C.-K. Min *et al.*, The Differentiation of Human Cytomegalovirus Infected-Monocytes Is Required for Viral Replication. **10** (2020).

1164 5. M. B. Reeves, P. A. MacAry, P. J. Lehner, J. G. P. Sissons, J. H. Sinclair, Latency, chromatin
1165 remodeling, and reactivation of human cytomegalovirus in the dendritic cells of healthy carriers.
1166 *Proceedings of the National Academy of Sciences of the United States of America* **102**, 4140 (2005).
1167 6. M. B. Reeves, J. H. Sinclair, Circulating dendritic cells isolated from healthy seropositive
1168 donors are sites of human cytomegalovirus reactivation in vivo. *J Virol* **87**, 10660-10667 (2013).
1169 7. J. Taylor-Wiedeman, J. G. P. Sissons, L. K. Borysiewicz, J. H. Sinclair, Monocytes are a major
1170 site of persistence of human cytomegalovirus in peripheral blood mononuclear cells. **72**, 2059-
1171 2064 (1991).
1172 8. E. Forte *et al.*, Tumor Necrosis Factor Alpha Induces Reactivation of Human
1173 Cytomegalovirus Independently of Myeloid Cell Differentiation following Posttranscriptional
1174 Establishment of Latency. *mBio* **9**, e01560-01518 (2018).
1175 9. C. Söderberg-Nauclér, K. N. Fish, J. A. Nelson, Reactivation of Latent Human
1176 Cytomegalovirus by Allogeneic Stimulation of Blood Cells from Healthy Donors. *Cell* **91**, 119-126
1177 (1997).
1178 10. M. B. Reeves, T. Compton, Inhibition of inflammatory interleukin-6 activity via
1179 extracellular signal-regulated kinase-mitogen-activated protein kinase signaling antagonizes
1180 human cytomegalovirus reactivation from dendritic cells. *J Virol* **85**, 12750-12758 (2011).
1181 11. J. Buehler *et al.*, Opposing Regulation of the EGF Receptor: A Molecular Switch Controlling
1182 Cytomegalovirus Latency and Replication. *PLOS Pathogens* **12**, e1005655 (2016).
1183 12. M. P. Weekes *et al.*, Latency-Associated Degradation of the MRP1 Drug Transporter
1184 During Latent Human Cytomegalovirus Infection. *Science* **340**, 199 (2013).
1185 13. V. T. K. Le, M. Trilling, H. Hengel, The Cytomegaloviral Protein pUL138 Acts as Potentiator
1186 of Tumor Necrosis Factor (TNF) Receptor 1 Surface Density To Enhance
1187 ULb'-Encoded Modulation of TNF-α Signaling. *Journal of Virology* **85**,
1188 13260 (2011).
1189 14. C. Montag *et al.*, The Latency-Associated UL138 Gene Product of Human Cytomegalovirus
1190 Sensitizes Cells to Tumor Necrosis Factor Alpha (TNF-α) Signaling by Upregulating TNF-α Receptor
1191 1 Cell Surface Expression. **85**, 11409-11421 (2011).
1192 15. E. R. Albright, C. K. Mickelson, R. F. Kalejta, Human Cytomegalovirus UL138 Protein
1193 Inhibits the STING Pathway and Reduces Interferon Beta mRNA Accumulation during Lytic and
1194 Latent Infections. *mBio* **12**, e0226721-e0226721 (2021).
1195 16. S. H. Lee, E. R. Albright, J.-H. Lee, D. Jacobs, R. F. Kalejta, Cellular defense against latent
1196 colonization foiled by human cytomegalovirus UL138 protein. *Sci Adv* **1**, e1501164-e1501164
1197 (2015).
1198 17. M. Umashankar *et al.*, Antagonistic Determinants Controlling Replicative and Latent
1199 States of Human Cytomegalovirus Infection. *Journal of Virology* **88**, 5987 (2014).
1200 18. M. A. Rak *et al.*, Human Cytomegalovirus UL135 Interacts with Host Adaptor Proteins To
1201 Regulate Epidermal Growth Factor Receptor and Reactivation from Latency. **92**, e00919-00918
1202 (2018).
1203 19. J. Buehler *et al.*, Host signaling and EGR1 transcriptional control of human
1204 cytomegalovirus replication and latency. *PLOS Pathogens* **15**, e1008037 (2019).
1205 20. K. Caviness *et al.*, Complex Interplay of the UL136 Isoforms
1206 Balances Cytomegalovirus Replication and Latency. *mBio* **7**, e01986-01915 (2016).
1207 21. K. Caviness, L. Cicchini, M. Rak, M. Umashankar, F. Goodrum, Complex expression of the
1208 UL136 gene of human cytomegalovirus results in multiple protein isoforms with unique roles in
1209 replication. *J Virol* **88**, 14412-14425 (2014).
1210 22. I. Mikell *et al.*, HCMV miR-US22 down-regulation of EGR-1 regulates CD34+ hematopoietic
1211 progenitor cell proliferation and viral reactivation. *PLoS Pathog* **15**, e1007854 (2019).

1212 23. I. M. Min *et al.*, The Transcription Factor EGR1 Controls Both the Proliferation and
1213 Localization of Hematopoietic Stem Cells. *Cell Stem Cell* **2**, 380-391 (2008).
1214 24. D. Collins-McMillen, J. Kamil, N. Moorman, F. Goodrum, Control of Immediate Early Gene
1215 Expression for Human Cytomegalovirus Reactivation. *Frontiers in cellular and infection*
1216 *microbiology* **10**, 476 (2020).
1217 25. B. A. Krishna, A. B. Wass, C. M. O'Connor, Activator protein-1 transactivation of the major
1218 immediate early locus is a determinant of cytomegalovirus reactivation from latency. *Proc Natl*
1219 *Acad Sci U S A* **117**, 20860-20867 (2020).
1220 26. A. E. Hale *et al.*, FOXO transcription factors activate alternative major immediate early
1221 promoters to induce human cytomegalovirus reactivation. *Proc Natl Acad Sci U S A* **117**, 18764-
1222 18770 (2020).
1223 27. V. G. Kew, J. Yuan, J. Meier, M. B. Reeves, Mitogen and stress activated kinases act co-
1224 operatively with CREB during the induction of human cytomegalovirus immediate-early gene
1225 expression from latency. *PLoS Pathog* **10**, e1004195 (2014).
1226 28. L. B. Crawford *et al.*, Human Cytomegalovirus Encodes a Novel FLT3 Receptor Ligand
1227 Necessary for Hematopoietic Cell Differentiation and Viral Reactivation. *MBio* **9** (2018).
1228 29. M. H. Hancock *et al.*, Human Cytomegalovirus UL7, miR-US5-1, and miR-UL112-3p
1229 Inactivation of FOXO3a Protects CD34(+) Hematopoietic Progenitor Cells from Apoptosis.
1230 *mSphere* **6** (2021).
1231 30. E. Scotti *et al.*, Targeted disruption of the idol gene alters cellular regulation of the low-
1232 density lipoprotein receptor by sterols and liver x receptor agonists. *Mol Cell Biol* **31**, 1885-1893
1233 (2011).
1234 31. R. G. de Bruin *et al.*, Quaking promotes monocyte differentiation into pro-atherogenic
1235 macrophages by controlling pre-mRNA splicing and gene expression. *Nat Commun* **7**, 10846
1236 (2016).
1237 32. Y. Liu, M. Tingart, S. Lecouturier, J. Li, J. Eschweiler, Identification of co-expression
1238 network correlated with different periods of adipogenic and osteogenic differentiation of BMSCs
1239 by weighted gene co-expression network analysis (WGCNA). *BMC Genomics* **22**, 254 (2021).
1240 33. E. Scotti *et al.*, IDOL stimulates clathrin-independent endocytosis and multivesicular body-
1241 mediated lysosomal degradation of the low-density lipoprotein receptor. *Mol Cell Biol* **33**, 1503-
1242 1514 (2013).
1243 34. C. Hong *et al.*, The E3 ubiquitin ligase IDOL induces the degradation of the low density
1244 lipoprotein receptor family members VLDLR and ApoER2. *J Biol Chem* **285**, 19720-19726 (2010).
1245 35. N. Zelcer, C. Hong, R. Boyadjian, P. Tontonoz, LXR regulates cholesterol uptake through
1246 Idol-dependent ubiquitination of the LDL receptor. *Science* **325**, 100-104 (2009).
1247 36. M. H. Glickman, A. Ciechanover, The ubiquitin-proteasome proteolytic pathway:
1248 destruction for the sake of construction. *Physiological reviews* **82**, 373-428 (2002).
1249 37. C. M. Pickart, Back to the future with ubiquitin. *Cell* **116**, 181-190 (2004).
1250 38. J. Zhang, Q. Liu, Cholesterol metabolism and homeostasis in the brain. *Protein Cell* **6**, 254-
1251 264 (2015).
1252 39. L. Zhang, K. Reue, L. G. Fong, S. G. Young, P. Tontonoz, Feedback regulation of cholesterol
1253 uptake by the LXR-IDOL-LDLR axis. *Arterioscler Thromb Vasc Biol* **32**, 2541-2546 (2012).
1254 40. J. Gao *et al.*, The E3 ubiquitin ligase IDOL regulates synaptic ApoER2 levels and is
1255 important for plasticity and learning. *Elife* **6**, e29178 (2017).
1256 41. J. K. Nelson *et al.*, Deubiquitylase Inhibition Reveals Liver X Receptor-independent
1257 Transcriptional Regulation of the E3 Ubiquitin Ligase IDOL and Lipoprotein Uptake. *J Biol Chem*
1258 **291**, 4813-4825 (2016).
1259 42. Anonymous, Cytomegalovirus. *Am J Transplant* **4 Suppl 10**, 51-58 (2004).

1260 43. Y. Du, G. Zhang, Z. Liu, Human cytomegalovirus infection and coronary heart disease: a
1261 systematic review. *Virol J* **15**, 31-31 (2018).
1262 44. N. Gudleski-O'Regan, T. M. Greco, I. M. Cristea, T. Shenk, Increased expression of LDL
1263 receptor-related protein 1 during human cytomegalovirus infection reduces virion cholesterol and
1264 infectivity. *Cell Host Microbe* **12**, 86-96 (2012).
1265 45. Y. Xi, S. Harwood, L. M. Wise, J. G. Purdy, Human Cytomegalovirus pUL37x1 Is Important
1266 for Remodeling of Host Lipid Metabolism. *J Virol* **93** (2019).
1267 46. Y. Xi, L. Lindenmayer, I. Kline, J. von Einem, J. G. Purdy, Human Cytomegalovirus Uses a
1268 Host Stress Response To Balance the Elongation of Saturated/Monounsaturated and
1269 Polyunsaturated Very-Long-Chain Fatty Acids. *mBio* **12** (2021).
1270 47. Y. Yu, T. G. Maguire, J. C. Alwine, Human cytomegalovirus infection induces adipocyte-like
1271 lipogenesis through activation of sterol regulatory element binding protein 1. *J Virol* **86**, 2942-
1272 2949 (2012).
1273 48. Y. Yu, F. J. Pierciey, Jr., T. G. Maguire, J. C. Alwine, PKR-like endoplasmic reticulum kinase
1274 is necessary for lipogenic activation during HCMV infection. *PLoS Pathog* **9**, e1003266 (2013).
1275 49. D. Collins-McMillen *et al.*, Alternative promoters drive human cytomegalovirus
1276 reactivation from latency. *Proc Natl Acad Sci U S A* **116**, 17492-17497 (2019).
1277 50. D. Collins-McMillen *et al.*, Alternative promoters drive human cytomegalovirus
1278 reactivation from latency. *Proceedings of the National Academy of Sciences* **116**, 17492 (2019).
1279 51. M.-C. Arcangeletti *et al.*, Human cytomegalovirus reactivation from latency: validation of
1280 a "switch" model in vitro. *Virol J* **13**, 179-179 (2016).
1281 52. L.-F. Yee, P. L. Lin, M. F. Stinski, Ectopic expression of HCMV IE72 and IE86 proteins is
1282 sufficient to induce early gene expression but not production of infectious virus in
1283 undifferentiated promonocytic THP-1 cells. *Virology* **363**, 174-188 (2007).
1284 53. B. G. Weinshenker, S. Wilton, G. P. Rice, Phorbol ester-induced differentiation permits
1285 productive human cytomegalovirus infection in a monocytic cell line. *J Immunol* **140**, 1625-1631
1286 (1988).
1287 54. N. Wagenknecht *et al.*, Contribution of the Major ND10 Proteins PML, hDaxx and Sp100
1288 to the Regulation of Human Cytomegalovirus Latency and Lytic Replication in the Monocytic Cell
1289 Line THP-1. *Viruses* **7**, 2884-2907 (2015).
1290 55. C. H. Lee *et al.*, Factors affecting human cytomegalovirus gene expression in human
1291 monocyte cell lines. *Mol Cells* **9**, 37-44 (1999).
1292 56. M. Peppenelli, J. Buehler, F. Goodrum, Human Hematopoietic Long-Term Culture (hLTC)
1293 for Human Cytomegalovirus Latency and Reactivation. *Methods Mol Biol* **2244**, 83-101 (2021).
1294 57. R. N. Ramirez *et al.*, Dynamic Gene Regulatory Networks of Human Myeloid
1295 Differentiation. *Cell systems* **4**, 416-429.e413 (2017).
1296 58. F. O. Martinez, S. Gordon, M. Locati, A. Mantovani, Transcriptional Profiling of the Human
1297 Monocyte-to-Macrophage Differentiation and Polarization: New Molecules and Patterns of Gene
1298 Expression. *The Journal of Immunology* **177**, 7303 (2006).
1299 59. B. Fagerberg, J. Gnarpe, H. Gnarpe, S. Agewall, J. Wikstrand, Chlamydia pneumoniae but
1300 not cytomegalovirus antibodies are associated with future risk of stroke and cardiovascular
1301 disease: a prospective study in middle-aged to elderly men with treated hypertension. *Stroke* **30**,
1302 299-305 (1999).
1303 60. M. C. Pizzorno, G. S. Hayward, The IE2 gene products of human cytomegalovirus
1304 specifically down-regulate expression from the major immediate-early promoter through a target
1305 located near the cap site. *J Virol* **64**, 6154-6165 (1990).

1306 61. J. M. Cherrington, E. L. Khoury, E. S. Mocarski, Human cytomegalovirus ie2 negatively
1307 regulates alpha gene expression via a short target sequence near the transcription start site. *J*
1308 *Virol* **65**, 887-896 (1991).
1309 62. B. Liu, T. W. Hermiston, M. F. Stinski, A cis-acting element in the major immediate early
1310 (IE) promoter of human cytomegalovirus is required for negative regulation by IE2. *J Virol* **65**, 897-
1311 903 (1991).
1312 63. M. P. Macias, M. F. Stinski, An in vitro system for human cytomegalovirus immediate early
1313 2 protein (IE2)-mediated site-dependent repression of transcription and direct binding of IE2 to
1314 the major immediate early promoter. *Proc Natl Acad Sci U S A* **90**, 707-711 (1993).
1315 64. K. Caviness *et al.*, Complex Interplay of the UL136 Isoforms Balances Cytomegalovirus
1316 Replication and Latency. *mBio* **7**, e01986 (2016).
1317 65. S. D. Lee, P. Tontonoz, Liver X receptors at the intersection of lipid metabolism and
1318 atherogenesis. *Atherosclerosis* **242**, 29-36 (2015).
1319 66. B. A. Janowski *et al.*, Structural requirements of ligands for the oxysterol liver X receptors
1320 LXRalpha and LXRbeta. *Proc Natl Acad Sci U S A* **96**, 266-271 (1999).
1321 67. B. A. Janowski, P. J. Willy, T. R. Devi, J. R. Falck, D. J. Mangelsdorf, An oxysterol signalling
1322 pathway mediated by the nuclear receptor LXRα. *Nature* **383**, 728-731 (1996).
1323 68. D. J. Peet, B. A. Janowski, D. J. Mangelsdorf, The LXRs: a new class of oxysterol receptors.
1324 *Current Opinion in Genetics & Development* **8**, 571-575 (1998).
1325 69. L. Fagerberg *et al.*, Analysis of the human tissue-specific expression by genome-wide
1326 integration of transcriptomics and antibody-based proteomics. *Molecular & cellular proteomics :*
1327 *MCP* **13**, 397-406 (2014).
1328 70. I. Fernandez-Ruiz, P. Puchalska, C. A. Narasimhulu, B. Sengupta, S. Parthasarathy,
1329 Differential lipid metabolism in monocytes and macrophages: influence of cholesterol loading[S].
1330 *Journal of Lipid Research* **57**, 574-586 (2016).
1331 71. T. R. Cimato, B. A. Palka, J. K. Lang, R. F. Young, LDL Cholesterol Modulates Human CD34+
1332 HSPCs through Effects on Proliferation and the IL-17 G-CSF Axis. *PLOS ONE* **8**, e73861 (2013).
1333 72. P. K. Morgan, L. Fang, G. I. Lancaster, A. J. Murphy, Hematopoiesis is regulated by
1334 cholesterol efflux pathways and lipid rafts: connections with cardiovascular diseases: Thematic
1335 Review Series: Biology of Lipid Rafts. *Journal of Lipid Research* **61**, 667-675 (2020).
1336 73. O. Soehnlein, F. K. Swirski, Hypercholesterolemia links hematopoiesis with
1337 atherosclerosis. *Trends in endocrinology and metabolism: TEM* **24**, 129-136 (2013).
1338 74. J. M. Radley, S. Ellis, M. Palatsides, B. Williams, I. Bertoncello, Ultrastructure of primitive
1339 hematopoietic stem cells isolated using probes of functional status. *Experimental hematology* **27**,
1340 365-369 (1999).
1341 75. S. Shariatmadar *et al.*, Electronic volume of CD34 positive cells from peripheral blood
1342 apheresis samples. *Cytometry. Part B, Clinical cytometry* **74**, 182-188 (2008).
1343 76. M. P. Vacanti, A. Roy, J. Cortiella, L. Bonassar, C. A. Vacanti, Identification and initial
1344 characterization of spore-like cells in adult mammals. *Journal of cellular biochemistry* **80**, 455-460
1345 (2001).
1346 77. A. C. Calkin *et al.*, FERM-dependent E3 ligase recognition is a conserved mechanism for
1347 targeted degradation of lipoprotein receptors. **108**, 20107-20112 (2011).
1348 78. B. Liu *et al.*, Inhibition of Human Cytomegalovirus Particle Maturation by Activation of
1349 Liver X Receptor. *Front Microbiol* **13**, 846386-846386 (2022).
1350 79. Q. Wang *et al.*, Identification of interferon-γ as a new molecular target of liver X receptor.
1351 *Biochemical Journal* **459**, 345-354 (2014).
1352 80. B. Sainz, H. L. LaMarca, R. F. Garry, C. A. Morris, Synergistic inhibition of human
1353 cytomegalovirus replication by interferon-alpha/beta and interferon-gamma. *Virol J* **2**, 14 (2005).

1354 81. K. A. Kropp *et al.*, Reversible inhibition of murine cytomegalovirus replication by gamma
1355 interferon (IFN-γ) in primary macrophages involves a primed type I IFN-signaling subnetwork for
1356 full establishment of an immediate-early antiviral state. *Journal of virology* **85**, 10286-10299
1357 (2011).
1358 82. Y. Wang *et al.*, Pseudorabies Virus Inhibits Expression of Liver X Receptors to Assist Viral
1359 Infection. *Viruses* **14**, 514 (2022).
1360 83. P. T. Lange, C. Schorl, D. Sahoo, V. L. Tarakanova, Liver X Receptors Suppress Activity of
1361 Cholesterol and Fatty Acid Synthesis Pathways To Oppose Gammaherpesvirus Replication. *mBio*
1362 **9**, e01115-01118 (2018).
1363 84. P. T. Lange, C. N. Jondle, E. J. Darrah, K. E. Johnson, V. L. Tarakanova, LXR Alpha Restricts
1364 Gammaherpesvirus Reactivation from Latently Infected Peritoneal Cells. *Journal of virology* **93**,
1365 e02071-02018 (2019).
1366 85. J. Zeng *et al.*, Liver X receptors agonists impede hepatitis C virus infection in an Idol-
1367 dependent manner. *Antiviral Res* **95**, 245-256 (2012).
1368 86. S. Bocchetta *et al.*, Up-regulation of the ATP-binding cassette transporter A1 inhibits
1369 hepatitis C virus infection. *PLoS One* **9**, e92140 (2014).
1370 87. H. Jiang *et al.*, Retinoic acid and liver X receptor agonist synergistically inhibit HIV infection
1371 in CD4+ T cells by up-regulating ABCA1-mediated cholesterol efflux. *Lipids Health Dis* **11**, 69
1372 (2012).
1373 88. L. Dubrovsky *et al.*, Liver X receptor agonist inhibits HIV-1 replication and prevents HIV-
1374 induced reduction of plasma HDL in humanized mouse model of HIV infection. *Biochem Biophys*
1375 *Res Commun* **419**, 95-98 (2012).
1376 89. T. M. Hanley, G. A. Viglianti, Nuclear receptor signaling inhibits HIV-1 replication in
1377 macrophages through multiple trans-repression mechanisms. *J Virol* **85**, 10834-10850 (2011).
1378 90. X. X. Sheng *et al.*, The LXR ligand GW3965 inhibits Newcastle disease virus infection by
1379 affecting cholesterol homeostasis. *Arch Virol* **161**, 2491-2501 (2016).
1380 91. J. Zeng *et al.*, Liver X receptors agonists impede hepatitis C virus infection in an Idol-
1381 dependent manner. *Antiviral Research* **95**, 245-256 (2012).
1382 92. G. H. Syed *et al.*, Hepatitis C virus stimulates low-density lipoprotein receptor expression
1383 to facilitate viral propagation. *Journal of virology* **88**, 2519-2529 (2014).
1384 93. A. Albecka *et al.*, Role of low-density lipoprotein receptor in the hepatitis C virus life cycle.
1385 *Hepatology (Baltimore, Md.)* **55**, 998-1007 (2012).
1386 94. S. Molina *et al.*, The low-density lipoprotein receptor plays a role in the infection of
1387 primary human hepatocytes by hepatitis C virus. *Journal of hepatology* **46**, 411-419 (2007).
1388 95. B. Sun *et al.*, Regulation of host and virus genes by neuronal miR-138 favours herpes
1389 simplex virus 1 latency. *Nature microbiology* **6**, 682-696 (2021).
1390 96. D. Pan *et al.*, A neuron-specific host microRNA targets herpes simplex virus-1 ICP0
1391 expression and promotes latency. *Cell Host Microbe* **15**, 446-456 (2014).
1392 97. X. Liu *et al.*, Herpesvirus-mediated stabilization of ICP0 expression neutralizes restriction
1393 by TRIM23. *Proc Natl Acad Sci U S A* **118** (2021).
1394 98. T. H. Chang *et al.*, Regulation of the Abundance of Kaposi's Sarcoma-Associated
1395 Herpesvirus ORF50 Protein by Oncoprotein MDM2. *PLoS Pathog* **12**, e1005918 (2016).
1396 99. J. C. Chmura *et al.*, The Itch ubiquitin ligase is required for KSHV RTA induced vFLIP
1397 degradation. *Virology* **501**, 119-126 (2017).
1398 100. E. S. Ehrlich, J. C. Chmura, J. C. Smith, N. N. Kalu, G. S. Hayward, KSHV RTA abolishes
1399 NFkappaB responsive gene expression during lytic reactivation by targeting vFLIP for degradation
1400 via the proteasome. *PLoS One* **9**, e91359 (2014).

1401 101. S. Gandon, Why Be Temperate: Lessons from Bacteriophage λ. *Trends in Microbiology* **24**,
1402 356-365 (2016).
1403 102. S. Atsumi, J. W. Little, Role of the lytic repressor in prophage induction of phage lambda
1404 as analyzed by a module-replacement approach. *Proceedings of the National Academy of Sciences*
1405 *of the United States of America* **103**, 4558-4563 (2006).
1406 103. R. A. Schubert, I. B. Dodd, J. B. Egan, K. E. Shearwin, Cro's role in the CI Cro bistable switch
1407 is critical for {lambda}'s transition from lysogeny to lytic development. *Genes Dev* **21**, 2461-2472
1408 (2007).
1409 104. M. G. Cortes, J. T. Trinh, L. Zeng, G. Balazsi, Late-Arriving Signals Contribute Less to Cell-
1410 Fate Decisions. *Biophys J* **113**, 2110-2120 (2017).
1411 105. O. Kobiler, A. Rokney, A. B. Oppenheim, Phage lambda CIII: a protease inhibitor regulating
1412 the lysis-lysogeny decision. *PLoS One* **2**, e363 (2007).
1413 106. J. W. Little, D. P. Shepley, D. W. J. T. E. j. Wert, Robustness of a gene regulatory circuit. **18**,
1414 4299-4307 (1999).
1415 107. J. D. Hernandez-Doria, V. Sperandio, Bacteriophage Transcription Factor Cro Regulates
1416 Virulence Gene Expression in Enterohemorrhagic Escherichia coli. *Cell Host Microbe* **23**, 607-
1417 617.e606 (2018).
1418 108. M. Umashankar *et al.*, A Novel Human Cytomegalovirus Locus Modulates Cell Type-
1419 Specific Outcomes of Infection. *PLOS Pathogens* **7**, e1002444 (2011).
1420 109. N. E. Sanjana, O. Shalem, F. Zhang, Improved vectors and genome-wide libraries for
1421 CRISPR screening. *Nat Methods* **11**, 783-784 (2014).
1422 110. X. Rao, X. Huang, Z. Zhou, X. Lin, An improvement of the 2^(-delta delta CT) method for
1423 quantitative real-time polymerase chain reaction data analysis. *Biostat Bioinforma Biomath* **3**, 71-
1424 85 (2013).
1425 111. J. Winer, C. K. Jung, I. Shackel, P. M. Williams, Development and validation of real-time
1426 quantitative reverse transcriptase-polymerase chain reaction for monitoring gene expression in
1427 cardiac myocytes in vitro. *Anal Biochem* **270**, 41-49 (1999).

1428

1429

1430

1431

1432

1433